Aalto University

Isogai, Akira; Hänninen, Tuomas; Fujisawa, Shuji; Saito, Tsuguyuki

Review: Catalytic oxidation of cellulose with nitroxyl radicals under aqueous conditions

Review: Catalytic oxidation of cellulose with nitroxyl radicals under aqueous conditions

Akira Isogai [a,*], Tuomas Hänninen [b], Shuji Fujisawa [a], Tsuguyuki Saito [a]

[a] Department of Biomaterials Science, Graduate School of Agricultural and Life Sciences, The University of Tokyo, Tokyo 113-8657, Japan
[b] Department of Forest Products Technology, Aalto University, PO Box 16300, FI-0076 Aalto, Espoo, Finland

ARTICLE INFO

ABSTRACT

2,2,6,6-Tetramethylpiperidine-1-oxyl radical (TEMPO)-mediated oxidation is a unique reaction to native and regenerated celluloses, and has advantages in terms of position-selective reaction at room temperature under aqueous conditions. When the TEMPO/NaBr/NaClO oxidation is applied to native celluloses in water at pH 10 under suitable conditions, the C6-primary hydroxy groups present on crystalline cellulose microfibril surfaces are mostly converted to sodium C6-carboxylate groups. Anionic sodium glucuronosyl units are densely, regularly, and position-selectively formed on crystalline cellulose microfibril surfaces, while maintaining the original cellulose morphology, cellulose I crystal structure, crystallinity, and crystal width. When TEMPO-oxidized celluloses (TOCs) prepared from, for example, wood cellulose have sodium C6-carboxylate contents >1 mmol/g, transparent highly viscous gels consisting of TEMPO-oxidized cellulose nanofibrils (TOCNs) with homogeneous widths of ≈3 nm and lengths >0.5 μm, dispersed at the individual nanofiber level, are obtained by gentle mechanical disintegration of TOCs in water. Alternative systems are as follows: TEMPO/NaClO/NaClO$_2$ system, TEMPO electro-mediated oxidation, etc. TOCNs are promising new plant-based renewable nanofibers applicable to high-tech material fields.

Contents

1. Introduction

Cellulose is a linear homopolysaccharide consisting of β-(1→4)-linked glucosyl units, each of which has one primary hydroxy group (C6–OH) and two secondary hydroxy groups (C2–OH and C3–OH). These hydroxy groups promote a hydrophilic nature of cellulosic materials. In addition, abundant C—H groups to the axial direction of glucosyl units in cellulose play a significant role in hydrophobic interactions between cellulose molecules and also between cellulose and other hydrophobic compounds in water (Fig. 1) [1,2]. Native celluloses form tightly packed crystal structures of cellulose I with various crystallinities and crystal sizes, in which numerous intra- and inter-molecular hydrogen bonds and hydrophobic interactions are regularly present [3–5]. The native cellulose I is further classified to two crystal structures of celluloses I$_\alpha$ and I$_\beta$, and most of terrestrial plant celluloses have cellulose I$_\beta$ [5,6].

Degrees of polymerization (DPs), or corresponding molar masses, of native celluloses vary from DP ≈800–≈5000, depending on cellulose resources used and isolation/purification conditions. Purity or α-cellulose content of native celluloses is also a significant factor, because non-cellulosic polysaccharides or hemicelluloses present in cellulosic materials can influence chemical reactions and properties of end products. Although the definition of the chemical structure of cellulose is simple, as described above, the properties of commercially available and laboratory-prepared cellulose samples vary in terms of the crystal structure, crystallinity, crystal size, DP/DP distribution, purity, depending on the original plant resource, which should all be taken into account.

Cotton lint and cotton linters celluloses, ramie and sisal fibers, and bleached wood chemical pulps are commercially available as cellulose samples with the native cellulose I structure and DPs >800 [7]. Microcrystalline cellulose powders are industrially produced from the above wood celluloses or cotton linters by dilute acid hydrolysis, and have relatively high cellulose purities and high cellulose I crystallinities, but low DPs of 200–300 [7]. Regenerated cellulose fibers such as viscose rayon, lyocell, and cuprammonium rayon have cellulose II crystal structures with various crystallinities and DPs of 350–800 [7–9]. These regenerated celluloses are prepared from cellulose/NaOH/CS$_2$/water, cellulose/*N*-methylmorpholine-*N*-oxide/water, and cellulose/Cu(NH$_3$)$_4$(OH)$_2$/water solutions, respectively, by wet or wet/dry spinning [8,9]. Bacterial cellulose prepared by incubating *Acetobacter xylinum*, and algal and tunicate celluloses can be used in laboratory experiments after isolation and purification, and each of them has a unique crystal structure, crystallinity, crystal size of cellulose I, and high DP > 4000 [10].

Chemical reactions of cellulose have been intensively and extensively studied to add new properties or functions to native celluloses, and some of them have already been used at the industrial level to produce cellulose derivatives, and their films and fibers [4,5,11–14]. Cellulose triacetate, cellulose diacetate, and cellulose nitrate are typical cellulose esters used as functional films or cellulose-based manmade fibers. Carboxymethylcellulose, methylcellulose, and hydroxyethyl- and hydroxypropyl-celluloses are water-soluble cellulose ethers used as stable thickeners.

The typical cellulose reactions such as esterification and etherification are condensations mostly in the presence of organic solvents, which generally require high temperatures for long reaction times. The presence of water in the starting cellulosic materials or in reaction media causes, therefore, preferential side reactions formed between water and an etherifying or esterifying reagent rather than reactions between cellulose hydroxy groups and reagents [4,5]. The reaction efficiencies between cellulose and these reagents are generally low, and simultaneously large amounts of reaction effluents containing byproducts, and other residual chemicals and solvents that require treatment are formed. These cellulose reactions are not environmentally friendly under their present conditions. Although a huge number of publications detailing chemical reactions of cellulose or preparation methods of cellulose derivatives have been reported, only limited cellulose derivatives are industrially produced at present. Some breakthrough processes, such as catalytic reactions at ambient temperatures under aqueous conditions like enzymatic reactions in living bodies, should be developed for further utilizations of chemically modified celluloses. The *N*-oxyl radical-mediated oxidation using, for example, 2,2,6,6-tetramethylpiperidine-1-oxyl (TEMPO) is one of the promising candidates in new cellulose reactions fitting to the above purpose.

Cellulose is advantageous as the most abundantly present and renewable biomass on the earth. Plants adsorb CO$_2$ and simultaneously emit O$_2$ (or proceed the reduction of CO$_2$, producing carbon-containing plant components and O$_2$) by photosynthesis during growing stage. The effective and continuous cycling of plantation, logging, utilization of plant biomass as materials, and their recycling can, therefore, reduce CO$_2$ in the atmosphere and subsequently retard global warming. The enhancement of qualitative and quantitative utilization of plant cellulose is the key issue for establishment of a sustainable society, partly in place of the present fossil resource-based society.

Overhead view
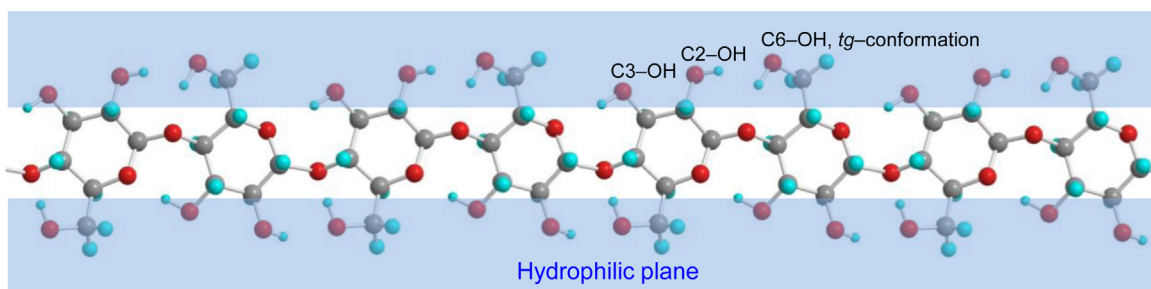
Side view
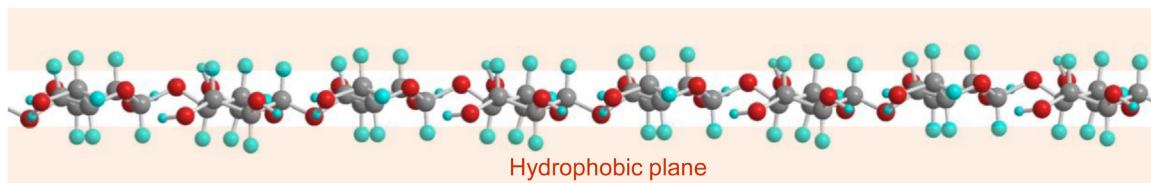
Fig. 1. Hydrophilic and hydrophobic planes of cellulose molecules, marked with the primary C6–OH (with *tg*-conformation corresponding to cellulose I crystal structure), and secondary C2–OH and C3–OH groups in glucosyl unit.

2. Introduction of carboxy groups into cellulose

Carboxy groups are typical functional moieties, and there are three conventional methods to introduce carboxy groups to cellulose: 1) carboxymethylation of cellulose with monochloroacetic acid and ≈20% NaOH with 2-propanol to form cellulose-OCH_2COONa, 2) N_2O_4 oxidation of gauze in chloroform to prepare fabrics with C6-carboxy groups, and 3) periodate oxidation of cellulose in water to prepare 2,3-dialdehyde cellulose followed by post-oxidation with $NaClO_2$ to form 2,3-dicarboxycellulose (Fig. 2). Although the carboxymethylation and N_2O_4 oxidation have been used at the industrial level, these reactions are not favourable in terms of reaction efficiency, position selectivity, chemical safety, and environmental issues. Water-soluble carboxymethylcellulose with degrees of substitution of 0.8–1.2 has been industrially produced and used as stable and safe thickeners as food additives, cosmetics, toothpastes, medicines, emulsion stabilizers, etc. Oxidation of viscose rayon gauze with N_2O_4 in chloroform has been used to produce commercial haemostat fabrics in surgical operation [15–21]. 2,3-Dialdehyde celluloses are prepared in laboratory by oxidizing cellulose with periodate ions in water at room temperature [22–31].

3. TEMPO-mediated oxidation of cellulose and other polysaccharides

3.1. Chemistry of TEMPO-mediated oxidation

de Nooy et al. first reported that catalytic reactions using TEMPO radical can position-selectively oxidize C6-primary hydroxy groups of water-soluble starch, pullulan, and dextran to sodium C6-carboxylate groups in water at pH 10 and ambient temperatures in the presence of NaBr and NaClO, which are used as a co-catalyst and a primary oxidant, respectively [32]. TEMPO is a water-soluble, stable, and commercially available *N*-oxyl radical with the Ames Test negative data (Ames Test: a fast and sensitive assay of the ability of a chemical compound or mixture to induce mutations in DNA) [33]. The TEMPO-mediated oxidation has opened a new research field of polysaccharide chemistry, because this reaction is different from conventional esterification, etherification, and oxidation of cellulose in terms of reaction efficiency and position selectivity under aqueous and moderate reaction conditions.

The TEMPO/NaBr/NaClO oxidation of saccharides and other compounds has been extensively studied for selective conversion of primary hydroxy groups to carboxy groups [34–36]. In this system, NaClO used as a primary oxidant first oxidizes TEMPO radical to the *N*-oxoammonium-type structure or TEMPO⁺, which then oxidize primary hydroxy groups to carboxy groups through C6-aldehydes. The reduced TEMPO or *N*-hydroxy-TEMPO is then oxidized by NaBrO, which is formed from NaBr by oxidation with NaClO. Thus, TEMPO and NaBr behave as catalysts, and only inexpensive NaClO is consumed during the oxidation. Because acidic carboxy groups are formed by the oxidation, a small amount of 0.5 M NaOH solution is consumed to maintain the aqueous reaction medium at pH 10 (Fig. 3). A part of aldehydes are directly oxidized to carboxy groups with NaClO and/or NaBrO [32,37].

More detailed reaction mechanism for the selective oxidation of primary hydroxy groups is illustrated in Fig. 4 [38]. The cationic TEMPO⁺ ion reacts with dissociated primary hydroxy groups to form a covalent bond as an intermediate structure. Because of steric hindrance, TEMPO⁺ ions form the covalent bond with the dissociated primary hydroxy groups much more preferentially than secondary hydroxy groups. Moreover, the dissociation of primary hydroxy groups is enhanced under alkaline conditions so that the formation of covalent bonds proceeds more rapidly under alkaline conditions than neutral or acidic conditions. The cleavage of the covalent bonds forms aldehyde groups and *N*-hydroxy-TEMPO molecules. The hydration of aldehydes and successive dissociation of the hydroxy groups under alkaline conditions causes the next covalent bond formation with TEMPO⁺, resulting in the formation of carboxy groups and *N*-hydroxy-TEMPO molecules. The optimum pH in water at ≈10 to form carboxy groups from primary hydroxy groups in the TEMPO/NaBr/NaClO oxidation is probably caused by a balance between the following two factors. The degrees of dissociation of primary hydroxy groups are enhanced under alkaline conditions, whereas the frequency to form the covalent bonds between dissociated hydroxy groups and TEMPO⁺ rather than those between OH⁻ ions and TEMPO⁺ molecules is preferential under weakly alkaline conditions.
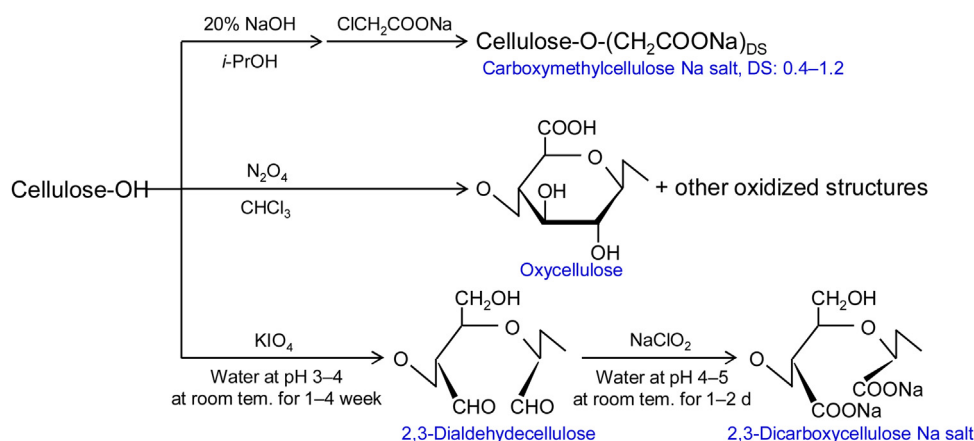
Fig. 2. Chemical reactions to introduce carboxy groups into cellulose molecule.
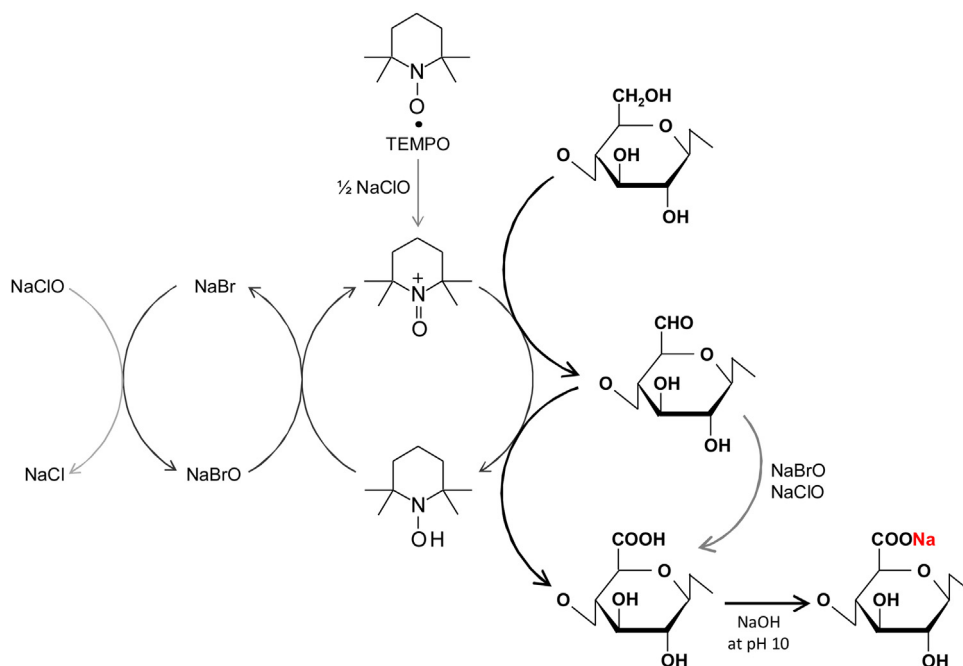
Fig. 3. Catalytic oxidation mechanism of C6–OH groups of cellulose by TEMPO/NaBr/NaClO in water at pH 10 [38].

3.2. Structures and properties of TEMPO-oxidized celluloses

When the TEMPO/NaBr/NaClO oxidation is applied to cellulose suspended in water at pH 10, it is possible to selectively convert C6–OH groups to sodium C6-carboxylate groups through C6-aldehydes (Fig. 3). If almost all C6–OH groups of water-insoluble cellulose are oxidized to sodium C6-carboxylate groups by oxidation, new water-soluble β-(1→4)-linked sodium polyglucuronates (or cellouronic acid Na salt) with homogeneous chemical structures should be obtained.

However, chemical structures and properties of TEMPO-oxidized products vary, depending on cellulose samples used as starting materials and the oxidation conditions. When regenerated celluloses, mercerized celluloses (prepared from native celluloses by soaking in NaOH solutions at >15% concentrations), and ball-milled/disordered cellulose powders are used as starting materials under suitable conditions, almost all C6–OH groups are oxidized to sodium C6-carboxylate groups to form water-soluble cellouronic acids Na salt (Fig. 5) [39–41]. However, the presence of small and unknown signals in ^{13}C NMR spectrum of sodium cellouronate

indicates some side reactions other than the oxidation of C6–OH groups.

Moreover, significant depolymerization is inevitable during the oxidation. The obtained cellouronic acids have DPs of ≈60, although the original celluloses used as starting materials have DPs >350 [41]. β-Alkoxy elimination occurring at C6-aldehyde groups formed as intermediate structures in water under alkaline conditions and/or some radical species formed in situ as byproducts during oxidation probably cause depolymerization [39,41–44].

Water-soluble sodium polyuronates with homogeneous chemical structures consisting of the same uronosyl repeating units are prepared from water-insoluble polysaccharides such as curdlan, paramylon, α-chitin, and starch, in a similar manner to that for sodium cellouronates [45–51]. Amine groups are unstable to the TEMPO-mediated oxidation; therefore, chitosan and proteins are degraded to water-soluble and low-molar-mass compounds, and position-selective oxidation of primary hydroxy groups in these polymers cannot be achieved [39]. When TEMPO-mediated oxidation is applied to native celluloses, consisting of crystalline cellulose microfibrils as the smallest elements next to cellulose chains, dif-
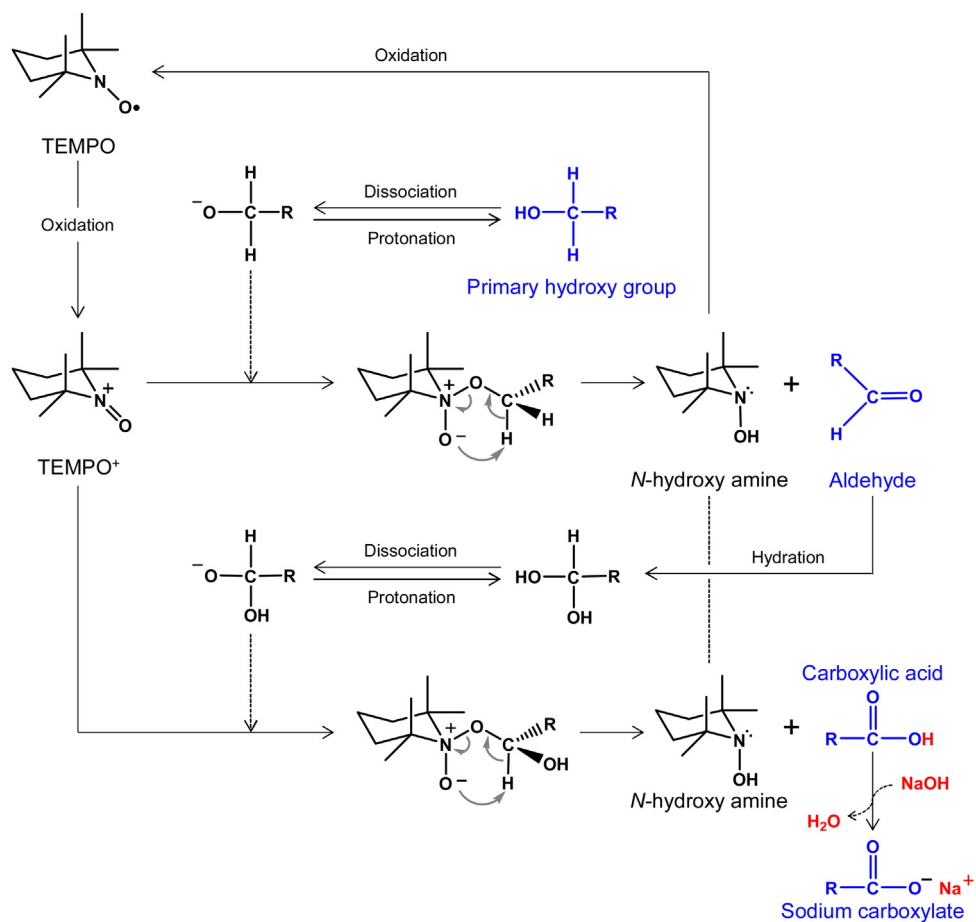
Fig. 4. TEMPO-mediated oxidation mechanism of primary hydroxyls to carboxyl groups via aldehydes [36,37]. The covalent bond formation between a dissociated primary hydroxyl group and cationized TEMPO⁺ is the initial key reaction.
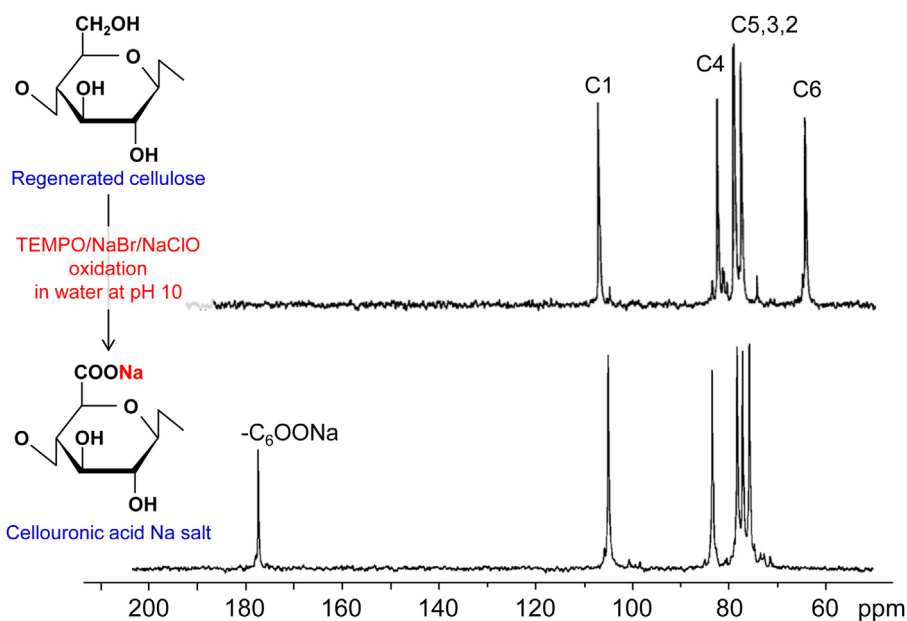
Fig. 5. Preparation of sodium β-(1→4)-poly(glucoronate) (or cellouronic acid Na salt) from regenerated cellulose by TEMPO-mediated oxidation, and ^{13}C NMR spectra of cellulose with DP 7 in DMSO-d_6 and cellouronic acid Na salt in D$_2$O [38,39]. The cellulose C6–OH signal at ≈62 ppm completely disappears, and the C6-carboxylate signal appears for the oxidized product.
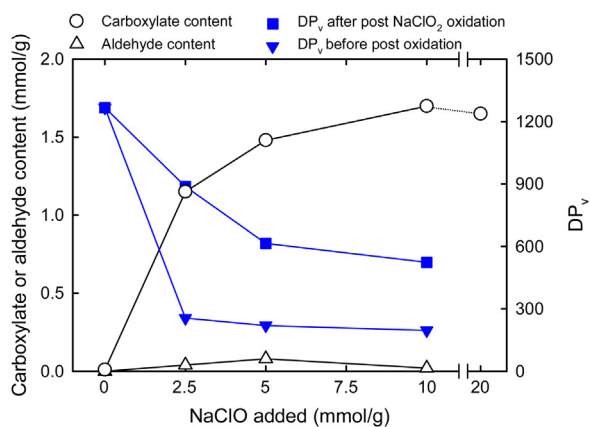
Fig. 6. Relationships between the amount of NaClO added and either carboxylate and aldehyde contents or DP_v values (before and after post oxidation with $NaClO_2$) of TEMPO-oxidized celluloses prepared from softwood bleached kraft pulp by TEMPO/NaBr/NaClO oxidation in water at pH 10 [38,60,108].

ferent oxidized products are obtained. Details are discussed in the following chapter.

4. Oxidation of native celluloses by TEMPO/NaBr/NaClO system

4.1. Structures and properties of TEMPO-oxidized native celluloses

When a commercial softwood bleached kraft pulp (papermaking grade), containing ≈90% cellulose and ≈10% hemicelluloses, is oxidized by the TEMPO/NaBr/NaClO system in water at pH 10, TEMPO-oxidized celluloses (TOCs) are obtained as water-insoluble products in the yields of ≈90%. The fibrous morphology, crystal structure of cellulose I, crystallinity, and crystal size of the original wood cellulose are maintained during the oxidation. Neutral sugar composition analysis have shown that mannose and xylose originating from hemicelluloses present in the wood cellulose are mostly removed from TOCs during the oxidation and washing processes. Carboxylate content of TOCs increases from 0.01 mmol/g up to ≈1.7 mmol/g with increasing the amount of NaClO added as the primary oxidant; a significant number of sodium C6-carboxylate groups are formed in TOCs (Fig. 6) [52–56]. Small amounts of aldehyde groups are present as intermediate structures in TOCs (Fig. 3).

When TOCs are dissolved in 0.5 M copper ethylenediamine [Cu(EDA)$_2$(OH)$_2$] (EDA: ethylenediamine) solution to determine their viscosity average DPs, TOCs have DPs lower than 300, which corresponds to the levelling-off DPs observed for plant celluloses by dilute acid hydrolysis [57–59]. However, after the TOCs are post-oxidized with $NaClO_2$ in water at pH 4–5, the TOCs have higher DPs >500. This is because small amounts of C6-aldehydes are formed and remain in the disordered regions periodically present along the cellulose microfibril direction in TOCs. These C6-aldehydes cause depolymerization of TOCs through β-alkoxy elimination in alkaline copper ethylenediamine solution during the DP measurement [60]. However, as shown in Fig. 6, even after post oxidation with $NaClO_2$, significant depolymerization is unavoidable during the TEMPO/NaBr/NaClO oxidation in water at pH 10 [60].

When TOCs are prepared from softwood and hardwood bleached kraft pulps, TOCs have the maximum sodium carboxylate contents of ≈1.7 mmol/g (Fig. 6). The maximum sodium carboxylate contents of TOCs depend on the original native celluloses used [38,61]. Fig. 7 shows the relationship between the maximum sodium C6-carboxylate content in TOCs and crystal width of cellulose I for various native celluloses used as starting materials [61].
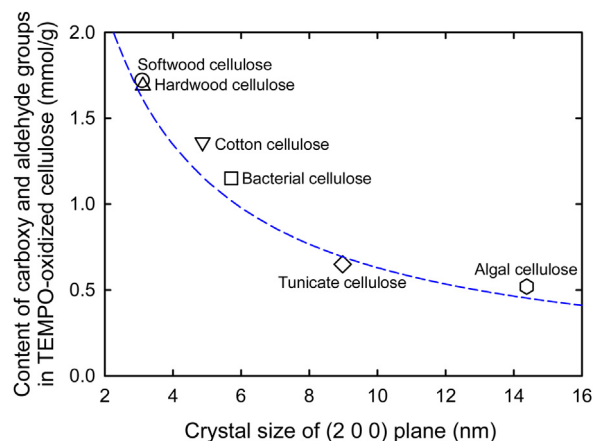

Fig. 7. Relationships between the (2 0 0) crystal size of cellulose I and maximum carboxylate content of TEMPO-oxidized celluloses prepared from various native celluloses. The dashed line shows relationship between crystal size and content of C6-OH groups present on surfaces of cellulose I crystallites. Crystal sizes were determined from X-ray diffraction patterns [61]. Copyright 2010. Reproduced with permission from the American Chemical Society.

Moreover, glucose/glucuronic acid alternating co-polysaccharides can be prepared from TOCs by surface peeling with aqueous NaOH (Fig. 8) [62].

These results show that almost all C6–OH groups present on crystalline cellulose microfibril surfaces in native celluloses are converted to sodium C6-carboxylate groups by TEMPO/NaBr/NaClO oxidation under suitable conditions. The high crystallinities and original crystalline microfibril structures of native celluloses cause a highly position-selective oxidation of C6–OH groups to sodium C6-carboxylate groups without oxidation of cellulose molecules inside the crystalline cellulose microfibrils (Fig. 9) [38,61–63]. Consequently, sodium C6-carboxylate groups are densely, regularly, and position-selectively formed on native cellulose microfibril surfaces by TEMPO/NaBr/NaClO oxidation, and abundantly present in TOCs. Other hypotheses concerning TEMPO-oxidized cellulose microfibril structures have been also proposed based on small-angle X-ray diffraction data [64–66].

Xylan-removed hardwood cellulose, bacterial cellulose, endo-type cellulase-pretreated nanocellulose films, lyocell fabrics, hemp, and other cellulosic materials have been oxidized by the TEMPO/NaBr/NaClO system in water at pH 10. Yields, carboxylate contents, crystal structures, and thermal properties of the obtained water-insoluble oxidized products have been studied in terms of reaction efficiency, depending on the starting native celluloses [67–75].

4.2. Kinetics of TEMPO-mediated oxidation of native cellulose

The conversion mechanism of the C6–OH groups exposed on crystalline cellulose microfibril surfaces of native celluloses to sodium C6-carboxylate groups by TEMPO/NaBr/NaClO oxidation in water at pH 10 are shown in Figs. 3 and 4, and the corresponding equation is shown in Fig. 10 [48]. The kinetics of oxidation of regenerated cellulose and lignin-containing mechanical pulp have been studied from carboxylate contents of the oxidized celluloses [75,76]. In the case of TEMPO/NaBr/NaClO oxidation of native celluloses, the kinetics can be studied indirectly by monitoring changes in NaClO concentration in the reaction media [70,77] or those of 0.5 M NaOH consumption to oxidation time [78]. The NaClO concentration in the reaction media can be determined by iodometric titration/UV–vis spectroscopy [77].

The effect of NaBr addition in TEMPO/NaClO oxidation of wood cellulose (1 g) in water at pH 10 on the formation rates of sodium
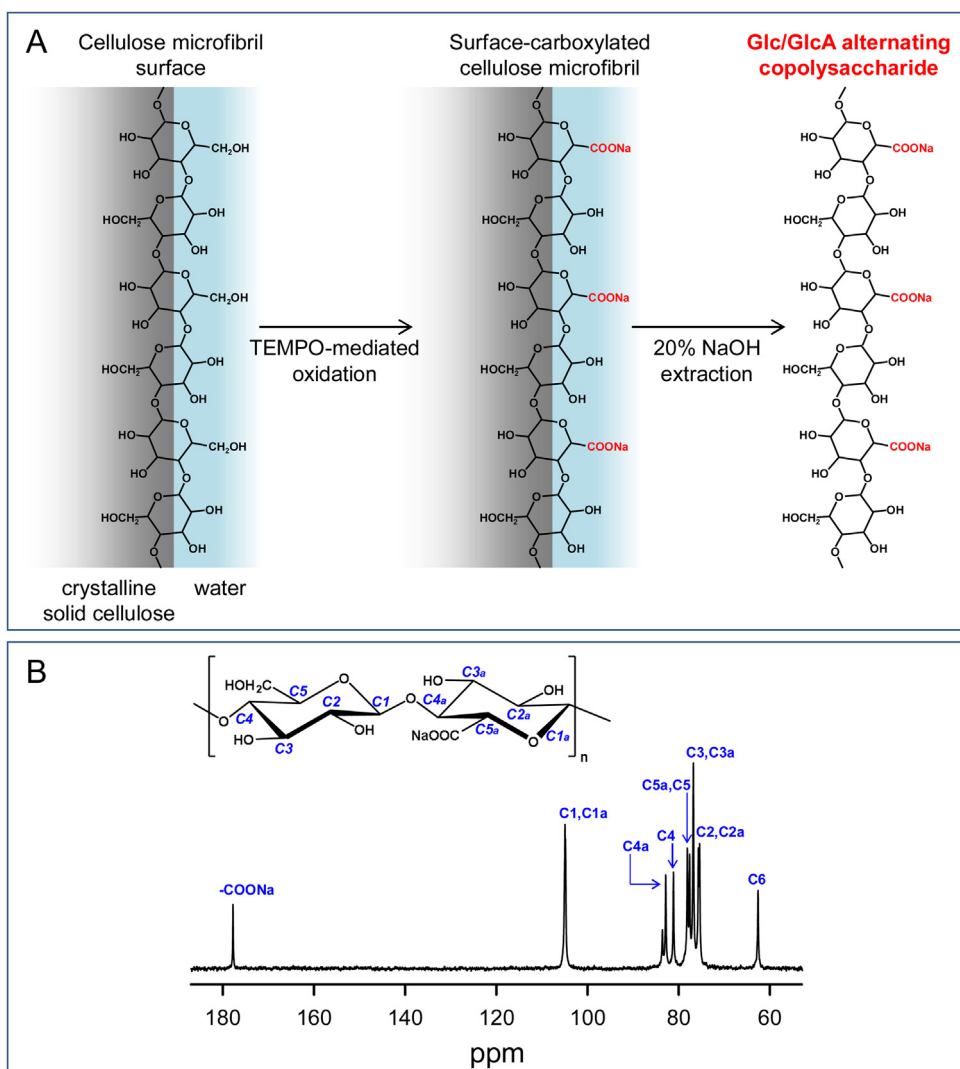
Fig. 8. Schematic model of glucose/glucuronic acid alternating co-polysaccharide prepared from surface peeling of TEMPO-oxidized native cellulose with aqueous NaOH (A). ^{13}C NMR spectrum of the obtained product (measured in D_2O) is also shown (B) [62].
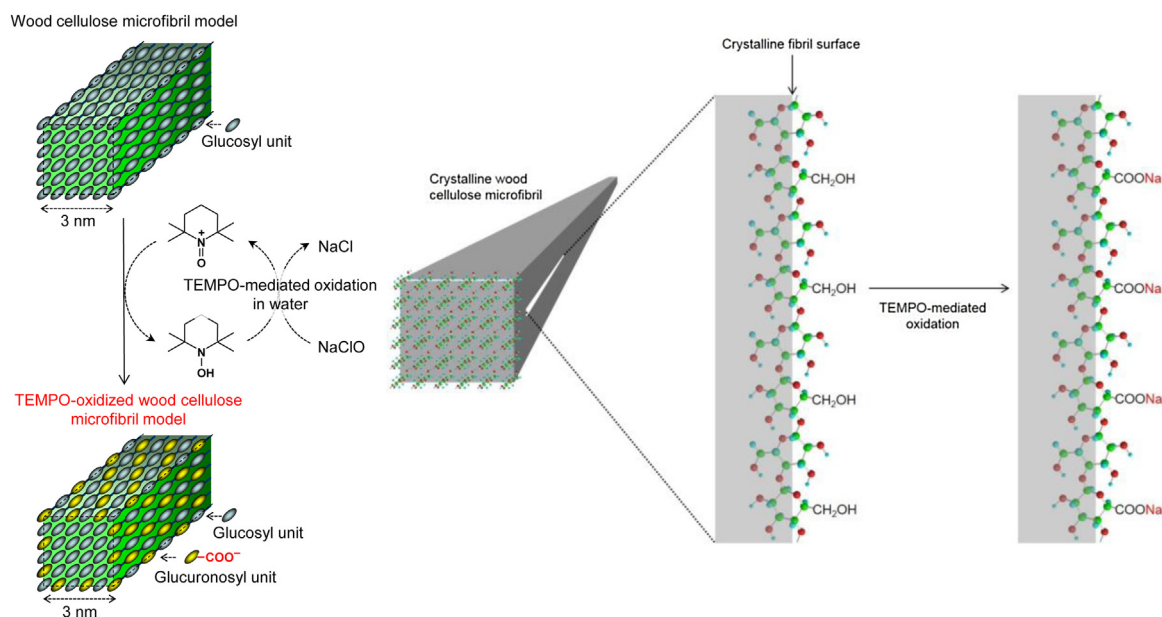
Fig. 9. Position-selective formation of sodium C6-carboxylate groups on crystalline cellulose microfibril surfaces by TEMPO-mediated oxidation of native cellulose [38,61,62]. Copyright 2010. Reproduced with permission from the American Chemical Society.
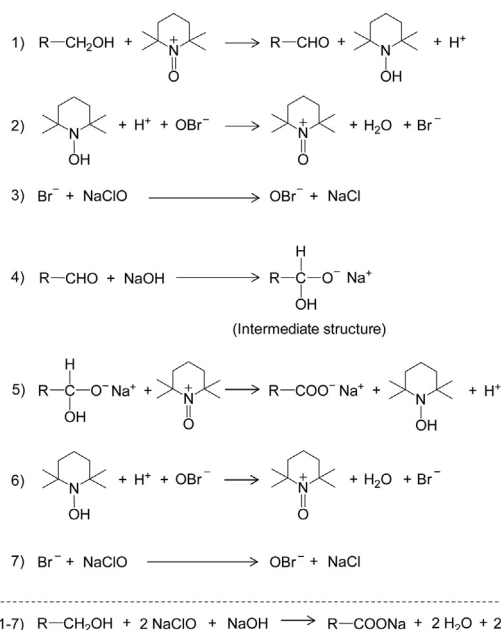
Fig. 10. Seven reaction formulae participating in catalytic oxidation of primary hydroxyl groups of polysaccharides to sodium C6-carboxylate groups by TEMPO/NaBr/NaClO system in water at pH 10 [48]. TEMPO and NaBr behave as catalysts; these two compounds are therefore not included in the equation below dotted line. Copyright 2003. Reproduced with permission from Elsevier Ltd.
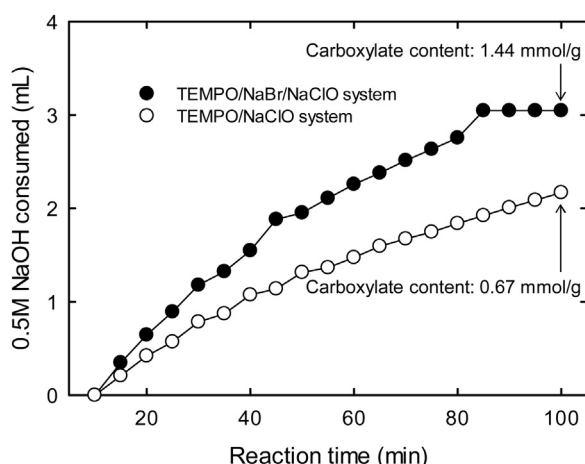
Fig. 11. Relationships between the oxidation time and the amount of 0.5 M NaOH consumed in TEMPO/NaBr/NaClO and TEMPO/NaClO oxidations of wood cellulose (1 g) in water at pH 10 [78]. The presence of NaBr as a co-catalyst remarkably improves the oxidation rate.

C6-carboxylate groups in oxidized celluloses was investigated by monitoring the amount of 0.5 M NaOH consumed (Fig. 11) [78]. According to the equation in Fig. 10, one mole of NaOH is consumed to form one mole of C6-carboxylate groups from one mole of C6 − OH groups. NaBrO is formed from NaClO and NaBr, and has much higher efficiency to oxidize TEMPO and N-hydroxy-TEMPO to TEMPO$^+$ than NaClO [32,35,39,79].

As shown in Fig. 11, the TEMPO/NaBr/NaClO-oxidized cellulose had a carboxylate content of 1.44 mmol/g after the 0.5 M NaOH consumption of 3.05 mL, which corresponds to 1.52 mmol NaOH. Therefore, ≈95% (= 1.44/1.52 × 100) of the added NaOH was consumed for the formation of sodium C6-carboxylate groups; the patterns of 0.5 M NaOH consumption can be used for calculation of oxidation kinetics. In the case of TEMPO/NaClO system, 1.09 mmol NaOH (or 2.17 mL of 0.5 M NaOH) was consumed to form sodium C6-carboxylate groups of 0.67 mmol/g; ≈38% (= 100 − 100 × 0.67/1.09) of the added NaOH was consumed in side reactions.

5. Preparation of TEMPO-oxidized cellulose nanofibrils and nanocrystals

5.1. TEMPO-oxidized cellulose nanofibrils (TOCNs)

When TOCs prepared from wood celluloses, cotton, cotton linters, algal, and tunicate celluloses have sufficient amounts of sodium C6-carboxylate groups, highly viscous transparent gels are obtained by gentle mechanical disintegration of TOC/water slurries [38,60,80–84]. An aqueous slurry of 0.1% (w/v) oxidized cellulose with a sodium carboxylate content of 1.5 mmol/g, prepared from hardwood cellulose by the TEMPO/NaBr/NaClO system in water at pH 10, has been stirred with a magnetic stirring bar at 500 rpm and room temperature (Fig. 12A). The originally fibrous wood TOC subsides at the bottom in the mixture before stirring. The TOC gradually swells in water by stirring, and a transparent dispersion with a 97% cellulose content in the supernatant fraction is obtained after stirring for 10 days [81]. The weight ratio of cellulose present in the supernatant fraction in Fig. 12A has been determined by centrifugation at 12 000g for 30 min to remove fibers or agglomerates present in the mixture.

The sodium carboxylate content of TOCs influences the transparency of the dispersions after mechanical disintegration in water. Fig. 12B shows photographs of a 0.1% (w/v) slurry of the original hardwood cellulose and 0.1% dispersions of hardwood TOCs with various carboxylate contents, after magnetic stirring in water for 10 days. The TOC with a carboxylate content of 1.0 mmol/g is homogeneously dispersed in water, but its dispersion is not transparent. On the other hand, a highly transparent gel can be obtained from the TOC with a carboxylate content of 1.5 mmol/g by disintegration in water under the same conditions.

When an ultrasonic homogenizer is used at the laboratory scale (in place of magnetic stirring in Fig. 12) for mechanical disintegration of the TOC with a carboxylate content of 1.5 mmol/g, transparent highly viscous gels are obtained within 8 min [60]. Disintegration of the TOC/water slurry using a laboratory-scale high-pressure homogenizer (such as Star Burst Labo HJP-25005, SUGINO, Japan) efficiently gives transparent gels within 4 cycles.

Transmission electron microscopy (TEM) images of the transparent wood TOC dispersions shown in Fig. 12, after dilution with water and air-drying on TEM grids, show that the dispersions consist of mostly individual cellulose fibrils with uniform lateral size of ≈3 nm and lengths >1 μm (the left low TEM image in Fig. 13) [81]. Vascular or terrestrial plant celluloses have crystalline microfibrils approximately 3 × 3 nm^2 cross-section in cell walls during biosynthesis [83,84]. Each cellulose microfibril consists of 30–40 fully extended cellulose chains. The TEM observation shows that the fibrous wood TOCs with 20–40 μm widths and 1–3 mm lengths are converted to individualized TOCNs with ≈3-nm widths and lengths >500 nm by gentle mechanical disintegration in water, when the sodium carboxylate contents of wood TOCs are ≈1 mmol/g or higher (Fig. 13).

As shown in Fig. 9, the sodium C6-carboxylate groups are position-selectively, densely, and regularly formed on crystalline cellulose microfibril surfaces in wood cellulose by TEMPO/NaBr/NaClO oxidation in water at pH 10. These surface anionic groups on cellulose microfibrils cause the complete individualization of cellulose microfibrils formed through osmotic effects and electrostatic repulsions efficiently working among surface anionic TOCN elements in water. High degrees of nanofibrillation for aqueous TOCN dispersions are confirmed from their high light
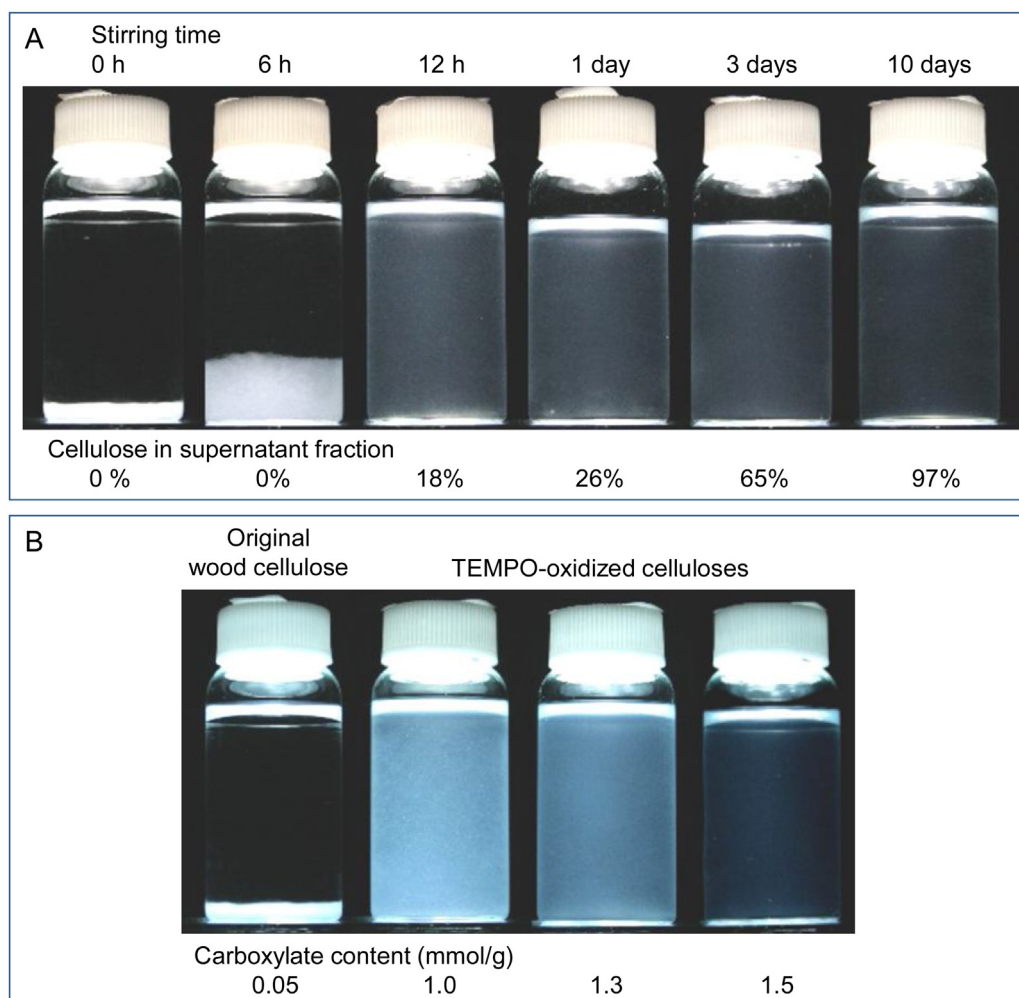
Fig. 12. Changes in the dispersion state of 0.1% (w/v) TEMPO-oxidized cellulose (TOC) in water with increased stirring time (A) and dispersion states of TOCs with different carboxylate contents, after stirring in water for 10 days (B) [81]. Copyright 2007. Reproduction with permission from the American Chemical Society.

transmittances without any light scattering (Fig. 14A) and birefringence behaviour by observation between cross-polarizers (Fig. 14B) [38,80,81,85].

Various plant holocelluloses are prepared from Japanese cedar (softwood), eucalyptus and birch (hardwood), ginkgo (gymnosperm), and rice straw and kenaf (grass) by repeated delignification with $NaClO_2$ in water at pH 4–5 and $\approx 70\,°C$. These holocelluloses are oxidized to TOCs with carboxylate contents of 1.3–1.7 mmol/g by TEMPO/NaBr/NaClO oxidation in water at pH 10. These TOCs are then converted to TOCNs with homogeneous ≈3-nm widths and high aspect (length/width) ratios >150 by gentle mechanical disintegration in water (Fig. 15 and Table 1) [86].

Softwood and hardwood celluloses [87–90], lignin-containing softwood thermomechanical pulp [91], and hemp bast, corn husk, cotton stark, palm tree, and other plant celluloses [92–98] have been oxidized to TOCs by the TEMPO/NaBr/NaClO system under various conditions. TOCNs prepared from the TOCs with sufficient amounts of carboxylate contents by gentle mechanical disintegration in water have been characterized. TOCNs with large widths of 5–15 nm are obtained from cotton, bacterial, tunicate, and algal celluloses by the oxidation and subsequent mechanical disintegration in water [80,99].

TOCs prepared from softwood bleached kraft pulp (papermaking grade) gives the highest efficiency to prepare TOCNs, when TOCs are prepared by the TEMPO/NaBr/NaClO oxidation and subsequent mechanical disintegration in water under the same conditions.

Aqueous 0.1% (w/v) TOCN dispersions prepared from softwood bleached kraft pulp have the highest transmittance (>90%) to visible light with wavelengths ranging 400–800 nm and the highest nanofibrillation yield (>90%), which is determined from dry weight of unfibrillated or partly fibrillated fraction present in the TOCN/water dispersion separated by centrifugation. Glucomannan molecules, i.e., predominant hemicelluloses in softwood cellulose, have $C6 - OH$ groups; therefore, 10–15% hemicelluloses in softwood cellulose are preferentially degraded to water-soluble and low-molar-mass compounds during TEMPO-mediated oxidation, resulting in the formation of almost pure water-insoluble TOCs, consisting of only glucosyl and glucuronosyl units. Because hardwood celluloses and hardwood holocelluloses contain hydrophobic xylan as a predominant hemicellulose, a part of xylan remains in TOCs, resulting lower light transmittances of TOCN/water dispersions and lower nanofibrillation yields [88,100].

5.2. TEMPO-oxidized cellulose nanocrystals (TO-CNCs)

When wood TOCs with carboxylate contents of 1.2–1.7 mmol/g are sonicated in water for an extended time such as totally 60–120 min with sufficient intervals to maintain the dispersion temperatures at 20–25 °C, needle-like TO-CNCs are obtained in the yields of ≈94% based on the starting wood cellulose weight (Fig. 16). These TO-CNCs have average lengths of 150–200 nm, homogeneous widths of ≈3 nm, and the same sodium carboxylate
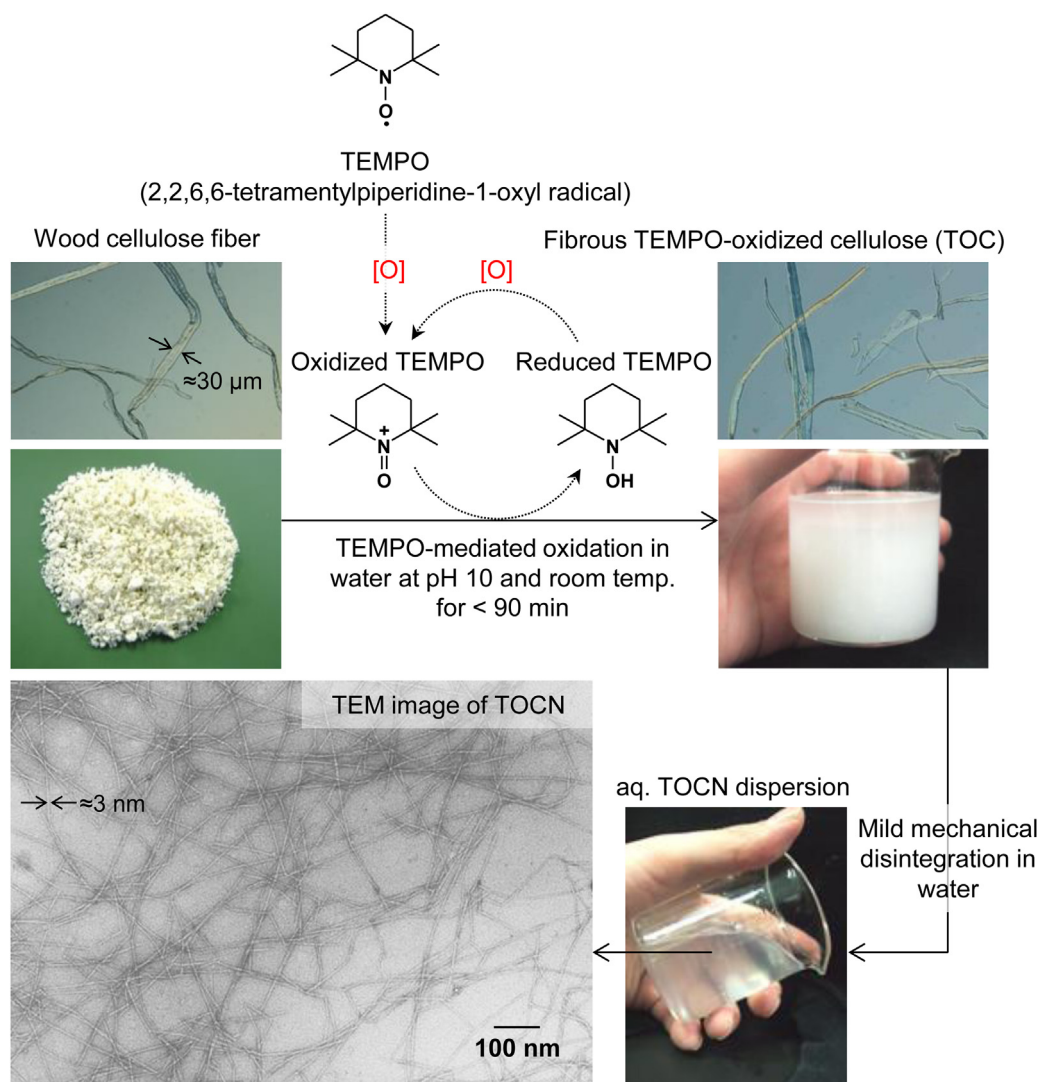
Fig. 13. Preparation of TEMPO-oxidized cellulose nanofibrils (TOCNs) dispersed in water from fibrous TEMPO-oxidized wood celluloses by mechanical disintegration [38,81].

Table 1
Average widths (nm) of TEMPO-oxidized cellulose nanofibrils prepared from various plant holocelluloses, determined from the AFM height images in Fig. 15 [86].

Sample	Ginkgo	Japanese cedar	Eucalyptus	Birch	Rice straw	Kenaf
Number-average width	3.11 ± 0.38	3.10 ± 0.39	3.12 ± 0.36	3.11 ± 0.42	3.08 ± 0.32	3.13 ± 0.30
Width-average width	3.15	3.14	3.16	3.16	3.11	3.16

contents of 1.2–1.7 mmol/g on the surfaces as those of the original TOCs [101]. Conventional CNCs are prepared from wood, cotton, tunicate, and algal celluloses with ≈64% H_2SO_4 at 70 °C, followed by washing with water using centrifugation and dialysis [102]. In the case of conventional wood CNCs with sulfate ester contents of ≈0.3 mmol/g, the yields decrease to ≈40% by acid hydrolysis. These CNCs have spindle-like morphologies with widths of 10–20 nm [103]. Wood TO-CNCs are different from the conventional wood CNCs in terms of yields, sizes, surface charges, and morphologies. Both TOCNs and TO-CNCs are, therefore, prepared from TOCs by controlling sonication time in water.

6. Characterization of TEMPO-oxidized celluloses (TOCs) and TEMPO-oxidized cellulose nanofibrils (TOCNs)

Structural characterizations of TOCs and TOCNs are significant for their application as new plant-based renewable nanofibers to high-tech material fields. Establishment of suitable analytical protocols are, therefore, required both in academia and industry. Carboxy and aldehyde contents of TOCs and TOCNs are determined by conductivity titration before and after post-oxidation with $NaClO_2$ [53,54,60,104].

The C6-carboxy groups in TOCs and TOCNs can be position-selectively and completely converted to methyl ester groups with trimethylsilyldiazomethane. These carboxy groups-methylated TOCs and TOCNs as well as the original celluloses and holocelluloses are completely soluble in 8% (w/w) lithium chloride/N,N-dimethylacetamide (LiCl/DMAc) [105–107]. The DPs and DP distributions of TOCs and TOCNs can be then determined using a size-exclusion chromatography system attached with a multi-angle laser-light scattering (SEC-MALLS) detector. The carboxy groups-methylated TOC and TOCN solutions as well as cellulose and hemicellulose-containing holocellulose solutions are diluted to 1% (w/v) LiCl/DMAc and subjected to the SEC-MALLS analysis.
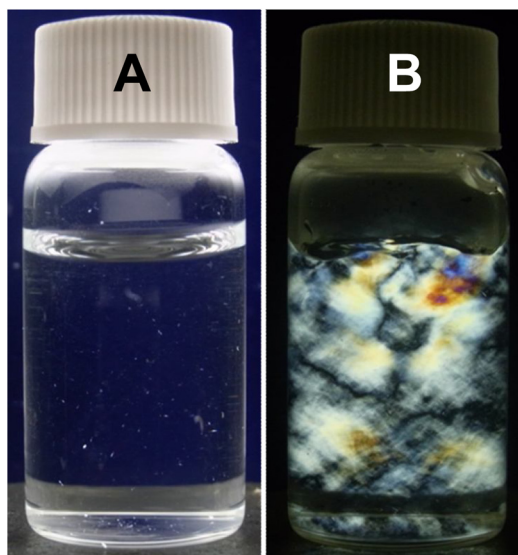
Fig. 14. Photographs of typical TEMPO-oxidized cellulose nanofibril (TOCN)/water dispersion (≈1%, ≈50 mL) consisting of completely individualized nanofibrils (A) and that observed between cross-polarizers (B). Clear birefringence is observed for the TOCN dispersion (B) without stirring because of nematic-ordered self-assembly behaviour of anionically charged TOCN elements in water.

The original softwood cellulose used as the starting material for preparation of TOCs has one major peak and a small shoulder peak in its molar-mass distribution, corresponding to cellulose-rich and hemicellulose-rich fractions, respectively. The peak top of TOCs shifts to the low-molar-mass direction, as the amount of NaClO added is increased (Fig. 17A) [108]. The shoulder peak originating from hemicelluloses becomes small and disappears as the amount of NaClO added is increased; hemicelluloses are preferentially degraded to water-soluble compounds during TEMPO/NaBr/NaClO

oxidation and removed from the water-insoluble TOCs. This is because plant hemicelluloses such as glucomannan and xylan have low DPs and disordered structures, different from cellulose, and are susceptible to degradation during oxidation.

When the fibrous TOC with a carboxylate content of 1.7 mmol/g (prepared from softwood cellulose) is sonicated in water, the average molar mass decreased with increasing sonication time in water (Fig. 17B) [108]. Significant depolymerization is, therefore, inevitable during the TEMPO/NaBr/NaClO oxidation and subsequent sonication in water.

Small amounts of C6-aldehyde groups and C2/C3 ketones are formed as side reactions in TOCs during TEMPO/NaBr/NaClO oxidation, and are present in TOCs and TOCNs. After post-reduction of TOCs with $NaBH_4$ in water at pH 8–10, intrinsic viscosities $[\eta]$ of TOCs obtained using 0.5 M copper ethylenediamine solution as the solvent are convertible to viscosity-average molar-masses (M_v) according to the Mark–Houwink–Sakurada equation of $[\eta]$ $(mL/g) = 0.094 \times M_v^{0.67}$, which is obtained from SEC-MALLS data for carboxy groups-methylated TOCs and TOCNs [108].

Crystallinities and crystal sizes of TOCs and TOCNs are determined from their X-ray diffraction patterns and solid-state ^{13}C NMR spectra. TEM and AFM are used to determine average widths of TOCNs. The length and length distribution of TOCNs are measured from TEM images, although only a limited number of TOCN elements (<300) is measurable in this case. Dilute TOCN/water dispersions consist of completely individualized TOCN elements without agglomeration. Therefore, rheological properties of TOCN/water dispersions have been studied to characterize TOCNs [8,109–111]. Average lengths of TOCNs prepared from wood, cotton linters, and algal celluloses under various conditions can be determined from shear viscosity behaviour of TOCN/water dispersions [110,111]. When intrinsic viscosities $[\eta]$ are obtained for various TOCNs and acid-hydrolyzed TOCNs, their average lengths are calculated using the following empirical formula, 1.6 $\times [\eta] = 0.15 \times p^{1.9}$, where p is the aspect ratio of TOCNs and acid-

Fig. 15. Atomic force microscopy (AFM) images of TEMPO-oxidized cellulose nanofibrils (TOCNs) prepared from various plant holocelluloses by TEMPO/NaBr/NaClO oxidation in water at pH 10 [86]. Copyright 2014. Reproduction with permission from Elsevier Ltd.

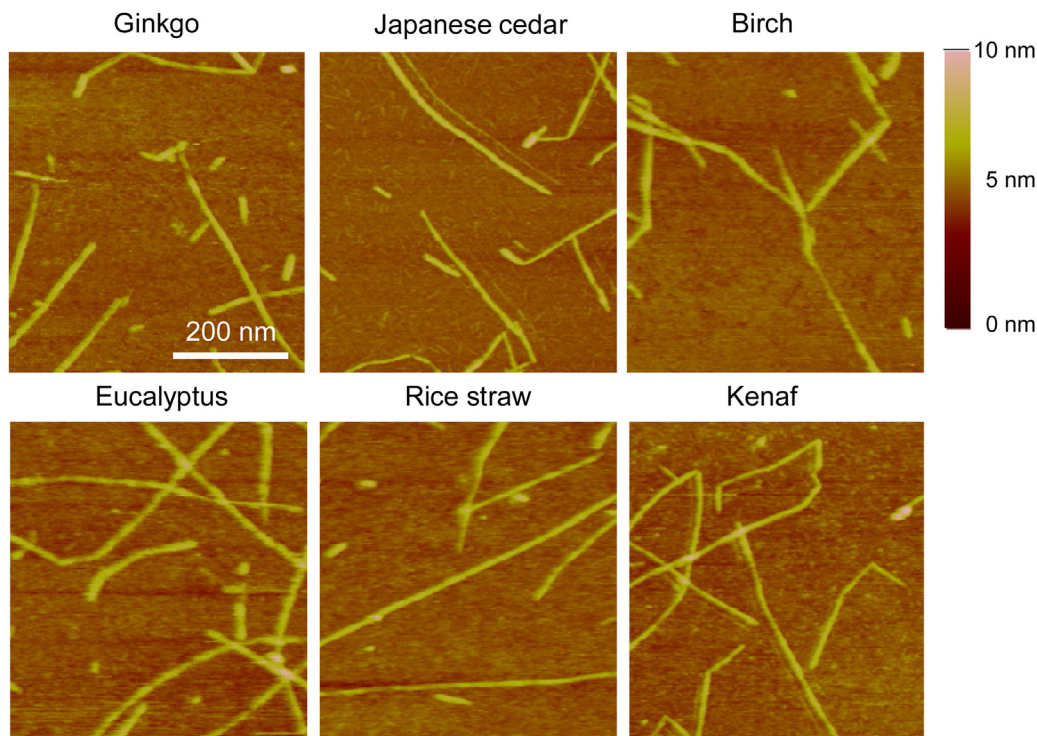TEMPO-mediated oxidation in water

Softwood bleached kraft pulp fiber

~3 μm

600 μm

Fibrous TEMPO-oxidized cellulose

600 μm

High-shear disintegration or long-time sonication in water

Gentle mechanical disintegration in water

Atomic force microscopy image

~3 nm

200 nm

TEMPO-oxidized cellulose nanocrystal

Transmission electron microscopy image

~3 nm

100 nm

TEMPO-oxidized cellulose nanofibril

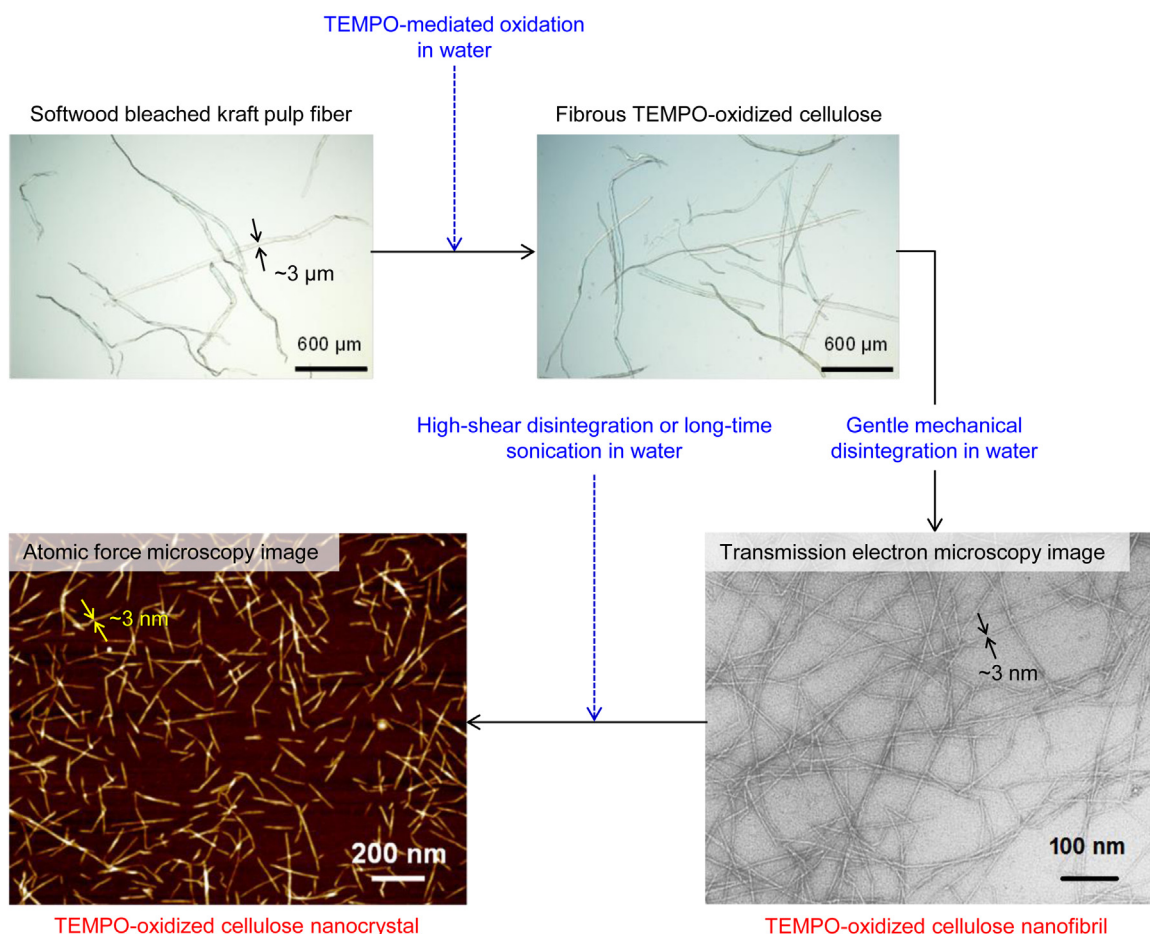**Fig. 16.** Preparation of TEMPO-oxidized cellulose nanofibers with lengths >500 nm and TEMPO-oxidized cellulose nanocrystals with lengths <200 nm from fibrous TEMPO-oxidized celluloses with carboxylate contents >1.2 mmol/g [101] by controlling disintegration conditions in water. Copyright 2018. Reproduction with permission from the American Chemical Society.

hydrolyzed TOCNs (Fig. 18) [111]. The p values are obtained as average lengths of hundreds of millions of TOCN elements present in dispersions; therefore, the length information obtained by the viscosity method is more reliable. However, no suitable method has been developed to date for determination of length distributions. The viscosity method cannot be applied to nanocelluloses with heterogeneous 3–100 nm widths that form network structures without dispersion at the individual nano-element level in water.

Average tensile strengths of TOCNs have been determined for aqueous TOCN dispersions by sonication or cavitation treatment and subsequent AFM analysis to measure limiting fracture lengths (or levelling-off and minimum lengths after sonication) and widths of TOCNs [112]. The validity of this cavitation method has been shown for carbon nanotubes, protein fibrils, and metal nanowires [113,114]. Wood and tunicate TOCNs have average tensile strengths of 1–6 GPa, when determined by the cavitation/AFM method [112]. These values are comparable with those of multi-walled carbon nanotubes and polyamide polymers such as Kevlar®, and much higher than that of steel although the density of TOCNs ($\approx$1.6 g/cm^3) is $\approx$1/5 that of steel. Tensile elastic moduli of TOCNs have been measured only for those prepared from tunicate cellulose with large microfibril widths from stress–strain curves obtained using a cantilever in AFM, and are $\approx$140 GPa [115]. TOCNs are, therefore, new plant-based renewable nanofibers with high mechanical strengths.

Agglomeration behaviour of aqueous TOCN dispersions in the presence of salts or cationic polymers, nanofibrillation of TOCs at high solid concentrations in water, swelling behaviour of TOCN

network structures in the presence of salts, simulations of TOCN structures in water, rheological behaviour of aqueous TOCN dispersions, and others have been studied to characterize TOCNs in water [116–122].

7. Effect of TEMPO-analogous compounds on oxidation efficiency of native cellulose

The effect of TEMPO derivatives and analogous compounds on oxidation efficiency of C6–OH groups of wood cellulose has been studied using the NaBr/NaClO system in water at pH 10 under the same conditions as those of TEMPO/NaBr/NaClO oxidation [123]. Among six- and five-membered N-oxyl radicals tested, 4-acetamido-TEMPO (4-AcNH-TEMPO) and 4-methoxy-TEMPO give TOCs with sufficiently high sodium C6-carboxylate contents (>1.1 mmol/g) after reaction for 4 h, and afford TOCN/water dispersions with high nanofibrillation yields when disintegrated in water under the same conditions. These two TEMPO derivatives can, therefore, be used as catalysts in place of TEMPO in oxidation of native celluloses with NaBr and NaClO in water at pH 10. The relationship between the sodium carboxylate content of TOCs prepared with various N-oxyl radicals and nanofibrillation yield is shown in Fig. 19 [123]. In contrast, 4-hydroxy-TEMPO and 4-oxo-TEMPO give the lowest efficiency in oxidation; the sodium C6-carboxylate contents of TOCs prepared with these TEMPO derivatives are lower than 0.3 mmol/g even after oxidation under the same conditions. The redox potentials of the TEMPO-analogous compounds in Fig. 19 have no correlation to the corresponding nanofibrillation yields
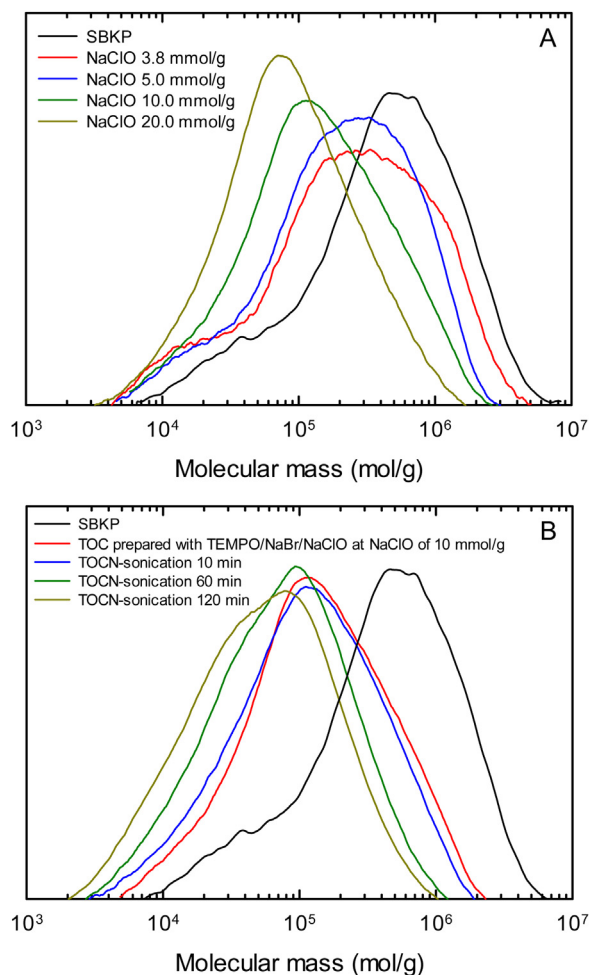
Fig. 17. Molar-mass distributions of the original softwood cellulose and TEMPO-oxidized celluloses (TOCs) prepared under various conditions (A) and those of TEMPO-oxidized cellulose nanofibrils (TOCNs) prepared from TOC by sonication for various times (B) Determined by SEC/MALLS analysis [108]. Copyright 2015. Reproduction with permission from the American Chemical Society.
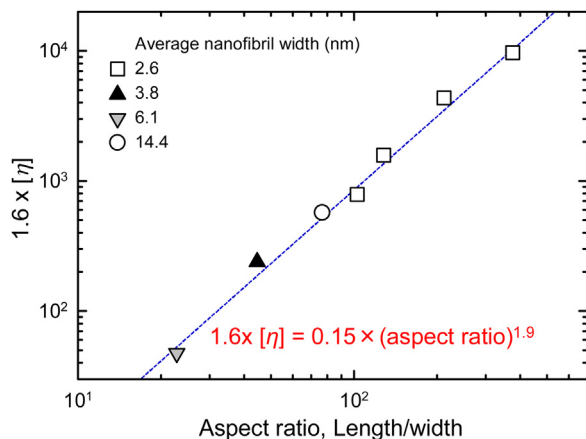
Fig. 18. Relationship between aspect ratio of various TEMPO-oxidized cellulose nanofibrils (TOCNs) and acid-hydrolyzed TOCNs measured from transmission electron microscopy (TEM) images and their intrinsic viscosities of aqueous dispersions [110]. These TOCNs and acid-hydrolyzed TOCNs are prepared from wood, cotton linters, and algal celluloses.
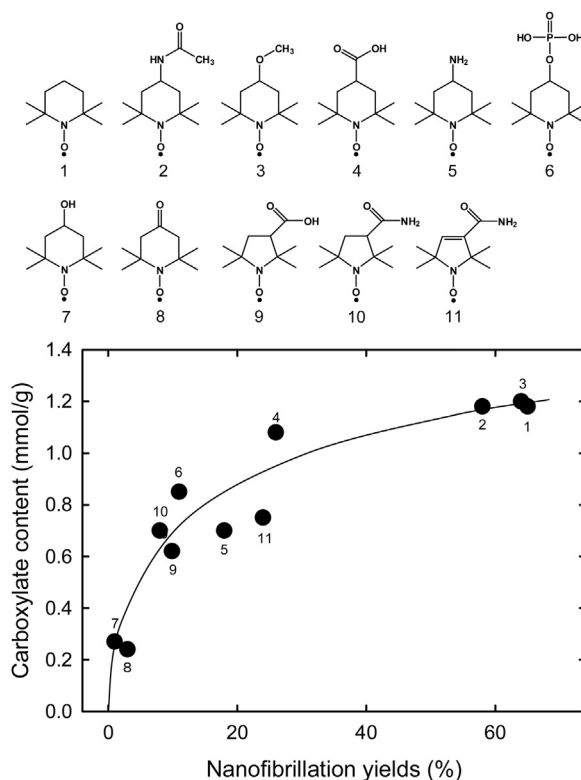
Fig. 19. Relationship between carboxylate content and nanofibrillation yield of TEMPO-oxidized wood celluloses prepared using TEMPO and its analogs by TEMPO/NaBr/NaClO oxidation in water at pH 10 [123]. Copyright 2010. Reproduced with permission from Elsevier Ltd.

of oxidized celluloses. Degradation behaviour or stability of the TEMPO-analogous compounds in water containing NaBr and NaClO primarily influences the resulting nanofibrillation yield of oxidized celluloses.

When wood cellulose is oxidized with the same amount of 2-azaadamantane N-oxyl (AZADO) or 1-methyl-AZADO as that of TEMPO in NaBr/NaClO system in water at pH 10, the oxidation time required for preparing oxidized celluloses with sodium C6-carboxylate contents of 1.2–1.3 mmol/g can be reduced from 80 to 10–15 min. The oxidation efficiency is, therefore, significantly improved using AZADO or 1-methyl-AZADO in place of TEMPO [124,125]. Moreover, the molar amounts of AZADO or 1-methyl-AZADO added for preparation of oxidized celluloses with sodium C6-carboxylate contents of 1.2–1.3 mmol/g can be reduced to 1/32 or 1/16 that of TEMPO, respectively, when the oxidation times are extended to 90 min as in the case of TEMPO/NaBr/NaClO oxidation. Almost no C6-aldehyde groups are formed in the oxidized celluloses.

The DP_v values of the AZADO- and 1-methyl-AZADO-oxidized celluloses, irrespective of their sodium C6-carboxylate contents, decrease from 1090 to ≈200, which is determined using 0.5 M copper ethylenediamine solution as the solvent. However, when the AZADO- or 1-methyl-ASADO-oxidized celluloses are post-reduced with $NaBH_4$, their DP_v values increase to 600–800. These results indicate that C2/C3 ketones are formed to some extent as side reactions in the oxidized celluloses.

The original crystallinity and crystal width of wood cellulose are unchanged after oxidation. The sodium C6-carboxylate groups and C2/C3 ketones formed as primary and side reactions, respectively, are present on crystalline cellulose microfibril surfaces. Highly transparent AZADO-oxidized cellulose nanofibril/water dispersions consisting of individually dispersed nanofibrils with a
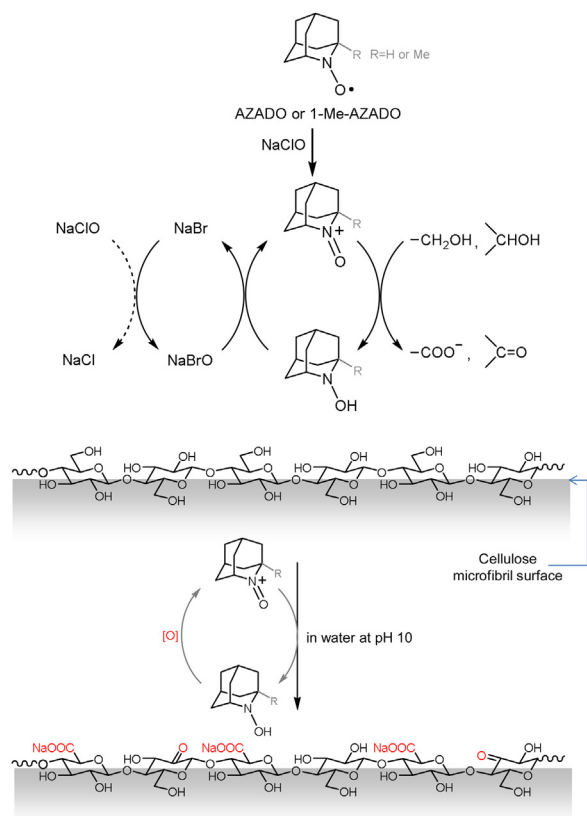
Fig. 20. Oxidation of primary and secondary hydroxy groups by AZADO/NaBr/NaClO or 1-Me-AZADO/NaBr/NaClO systems, and schematic model of AZADO- or 1-Me-AZADO-oxidized native cellulose [125]. Copyright 2013. Reproduction with permission from Springer Nature.

Fig. 21. Preparation of 2,3,6-tricarboxylate-cellulose from regenerated cellulose by AZADO/NaBr/NaClO oxidation in water at pH 10 [126]. Copyright 2014. Reproduction with permission from Elsevier Ltd.

nanofibrillation yield of 89% are obtained from the AZADO-oxidized cellulose with a sodium carboxylate content of 1.2 mmol/g by mechanical disintegration in water. The AZADO and 1-methyl-AZADO oxidations of cellulose microfibrils with NaBr/NaClO in water at pH 10 are schematically illustrated in Fig. 20 [125].

When a regenerated cellulose fiber (Bemliese®) is oxidized by AZADO/NaBr/NaClO in water at pH 10 under suitable conditions, water-soluble sodium 2,3,6-tricarboxylate cellulose (NaTCC) or sodium mesotartarate/monohydrated glyoxilate alternating co-polyacetal is obtained in a yield of 82% by one-step oxidation (Fig. 21) [126]. Almost all C6–OH groups are converted to sodium C6-carboxylate groups and also almost all the C—C bonds of C2/C3 are cleaved to form sodium C2- and C3-carboxylate groups by AZADO/NaBr/NaClO oxidation. The weight- and number-average molar-masses of the obtained NaTCC are 10,700 and 7000, respectively; the original DP_v (680) of regenerated cellulose decreases to weight- and number-average DPs (DP_w and DP_n, respectively) of 52 and 34, respectively, for the NaTCC [126]. When AZADO-mediated oxidation is applied to wood cellulose, water-soluble oxidized products are obtained. However, they have more heterogeneous chemical structures indicating that complete oxidation of the C2, C3, and C6 hydroxy groups to carboxy groups is difficult to achieve for wood cellulose [126].

8. TEMPO/NaClO/NaClO₂ oxidation of cellulose and other polysaccharides

The TEMPO/NaBr/NaClO oxidation in water at room temperature and pH 10 under suitable conditions efficiently converts native celluloses to TOCs with high sodium carboxylate contents within 90 min. However, significant depolymerization is inevitable
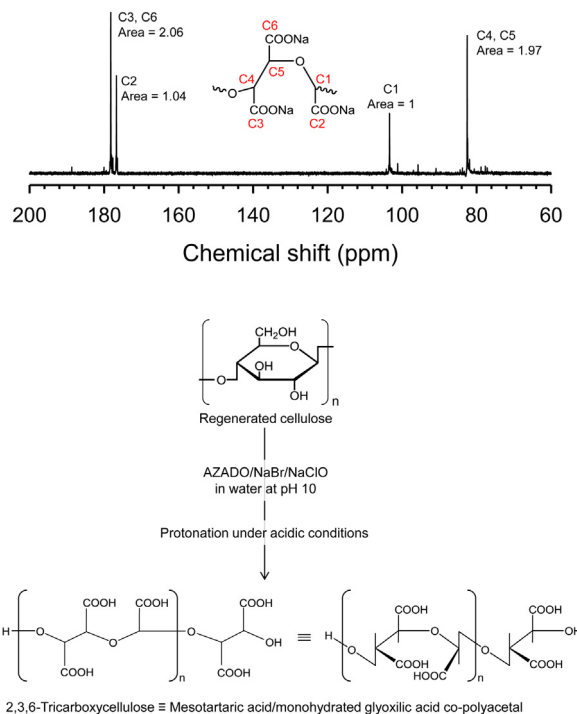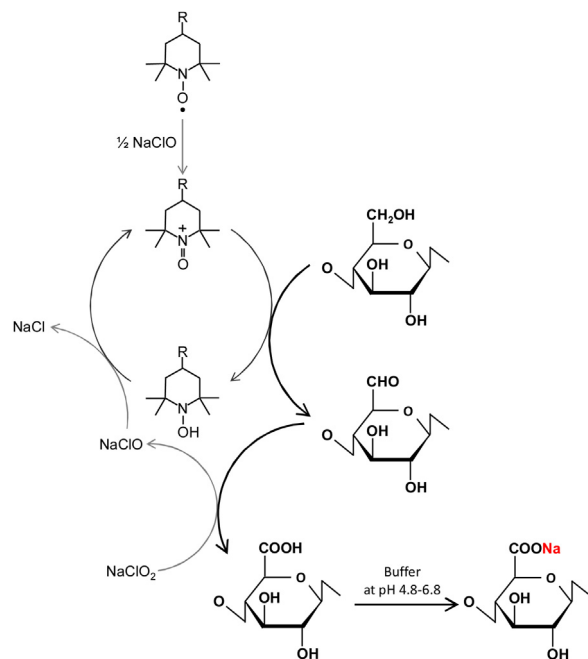
Fig. 22. Oxidation mechanism of C6–OH groups of cellulose by TEMPO/NaClO/NaClO₂ in buffer at pH 4.8 or 6.8 [38,127,128]. No C6-aldehydes are present in oxidized celluloses because oxidation of C6-aldehydes to C6-carboxys occurs with NaClO₂ present as the primary oxidant.

on cellulose and oxidized cellulose molecules in TOCs during the oxidation [60,108]. One of the alternative oxidation systems is TEMPO/NaClO/NaClO₂ in water at high temperatures under weakly acidic or neutral conditions for long times >1 d (Fig. 22). Here, TEMPO and NaClO behave as catalysts and NaClO₂ behaves as a primary oxidant to be consumed [127–130]. In this oxidation system, no C6-aldehyde groups are formed in TOCs, and depolymerization
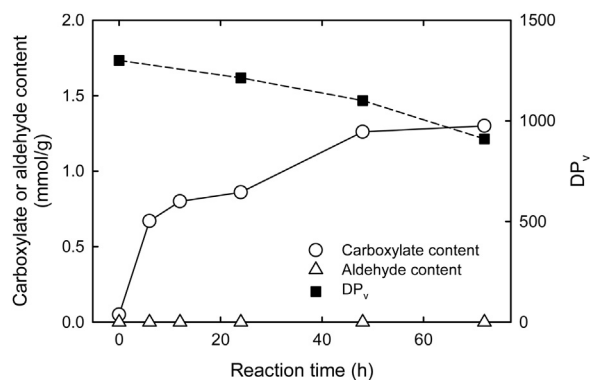
Fig. 23. Relationship between reaction time of wood cellulose by 4-acetamido-TEMPO/NaClO/NaClO$_2$ oxidation in buffer at pH 4.8 and 40 °C, and carboxylate and aldehyde contents, and viscosity average-degree of polymerization (DP$_v$) of TEMPO-oxidized wood celluloses [130]. Copyright 2012. Reproduction with permission from Elsevier Ltd.

of oxidized celluloses, caused by β-alkoxy elimination preferentially occurring under alkaline conditions, is avoidable.

When wood cellulose is oxidized by TEMPO/NaClO/NaClO$_2$ or 4-AcNH-TEMPO/NaClO/NaClO$_2$ system in a buffer at pH 4.8 or 6.8 and 40 °C for 2 d under suitable conditions, the sodium C6-carboxylate content in the TOCs increases up to ≈1.3 mmol/g. The DP$_v$ values of the obtained TOCs slightly decrease from 1270 for wood cellulose to ≈1100 during the oxidation (Fig. 23) [130]. Depolymerization is, therefore, mostly avoidable for TOCs prepared by TEMPO/NaClO/NaClO$_2$ oxidation in comparison with TEMPO/NaBr/NaClO oxidation in water at pH 10. The 4-AcNH-TEMPO is better than TEMPO in terms of high amounts of sodium C6-carboxylate groups introduced and high DP$_v$ values of the TOCs.

The original crystallinity and crystal width of cellulose I for wood cellulose are maintained during the oxidation, and transparent highly viscous gels are obtained by mechanical disintegration of the wood cellulose-derived TOCs, with sodium C6-carboxylate contents >0.8 mmol/g, in water [128,130]. Softwood cellulose gives aqueous TOCN gels with higher light transmittances than those from hardwood cellulose when mechanically disintegrated in water under the same conditions. The gels consist of mostly individualized TOCN elements with homogeneous ≈3-nm widths similar to those of TOCNs prepared by the TEMPO/NaBr/NaClO system in water at pH 10. However, the obtained TOCNs have higher average lengths >1 μm (Fig. 24) than those of TOCNs prepared by TEMPO/NaBr/NaClO oxidation [128,130].

The TEMPO/NaClO/NaClO$_2$ oxidation of water-insoluble curdlan with suitable amounts of NaClO$_2$ in a buffer at pH 4.8 or 6.8 gives the corresponding water-soluble sodium polyuronates with high DPs consisting of glucuronosyl repeating units are obtained in high yields [131,132]. However, when commercial regenerated cellulose fibers, beads for chromatographic use, and mercerized celluloses prepared from native cellulose by swelling with 20% aqueous NaOH under various conditions are used as starting materials for TEMPO/NaClO/NaClO oxidation in water at pH 4.8 and 60 °C, weight recovery ratios as water-insoluble fractions and their sodium C6-carboxylate contents are in the range 67–80% and 1.8–2.2 mmol/g, respectively [133–136]. The sodium C6-carboxylate content of water-soluble pure sodium cellouronates consisting of glucuronosyl repeating units is 5.05 mmol/g; therefore, the sodium carboxylate contents of water-insoluble fractions of oxidized regenerated cellulose fibers and beads, and mercerized celluloses are lower than that of sodium cellouronates. The water-insoluble fractions of the oxidized products are converted to almost transparent dispersions by mechanical disintegration in water, consisting of mostly individualized TEMPO-oxidized CNCs
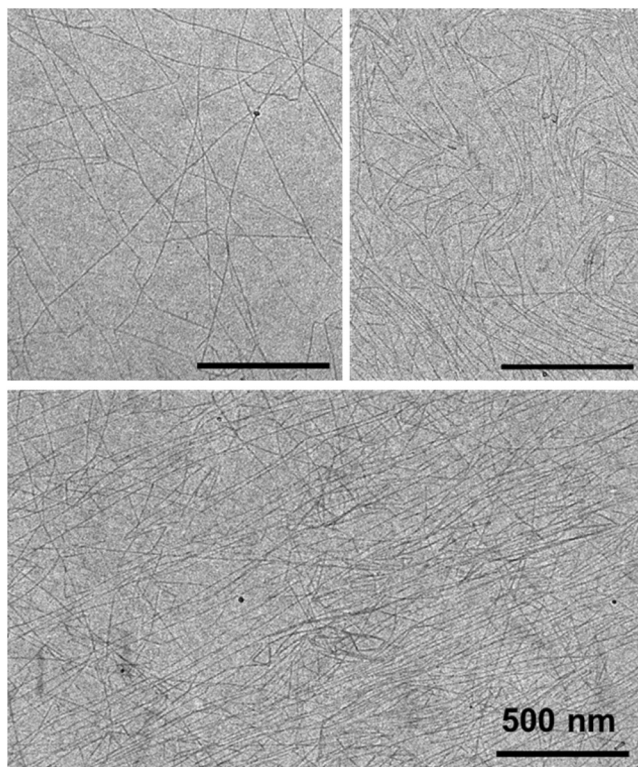
Fig. 24. Transmission electron microcopy (TEM) images of TEMPO-oxidized cellulose nanofibrils (TOCNs) with carboxylate content of 0.8 mmol/g, prepared from hardwood cellulose by TEMPO/NaClO/NaClO oxidation in buffer at pH 6.8 and 60 °C for 52 h. Observed by diffraction contrast method [128].

(Fig. 25) [135]. These results indicate that oxidation of C6–OH groups selectively occurs on cellulose II crystallite surfaces. The TEMPO/NaClO/NaClO$_2$ or 4-AcNH-TEMPO/NaClO/NaClO$_2$ oxidation has been applied to bacterial cellulose, alkali-treated wood cellulose, and cotton fabrics, and the oxidized products have been characterized [137–139].

9. TEMPO electro-mediated oxidation of cellulose

TEMPO electro-mediated oxidation is another alternative to TEMPO/NaBr/NaClO oxidation for cellulose in water under neutral conditions, in which no chlorine-containing reagents are needed for oxidation (Fig. 26) [140–147]. When the electro-mediated oxidation is applied to wood cellulose with TEMPO or 4-AcNH-TEMPO in a buffer at pH 6.8 and room temperatures for 2 d, the solid recovery ratio of the water-insoluble oxidized cellulose is more than 90%, and the sodium C6-carboxylate content increases to ≈0.9 mmol/g. A significant amount of C6-aldehyde groups (≈0.4 mmol/g) is formed simultaneously in the oxidized cellulose. The DP$_v$ value of wood cellulose decreases from 1270 to 810 during the oxidation (Fig. 27) [147]. The original cellulose I crystallinity and crystal width of wood cellulose are maintained after the oxidation, showing that all the sodium C6-carboxylate and C6-aldehyde groups are position-selectively formed on crystalline cellulose microfibril surfaces. The oxidized celluloses with carboxylate contents >0.9 mmol/g are convertible to TOCNs dispersed at the individual nanofibril level by disintegration in water, and nanofibrillation yields are more than 80%.

Sodium C6-carboxylate groups are predominantly formed in the oxidized celluloses prepared by the TEMPO electro-mediated oxidation without using NaClO. This result shows that the oxidized TEMPO or TEMPO$^+$ molecules can oxidize not only C6–OH groups to C6-aldehydes but also C6-aldehyde groups, formed as interme-
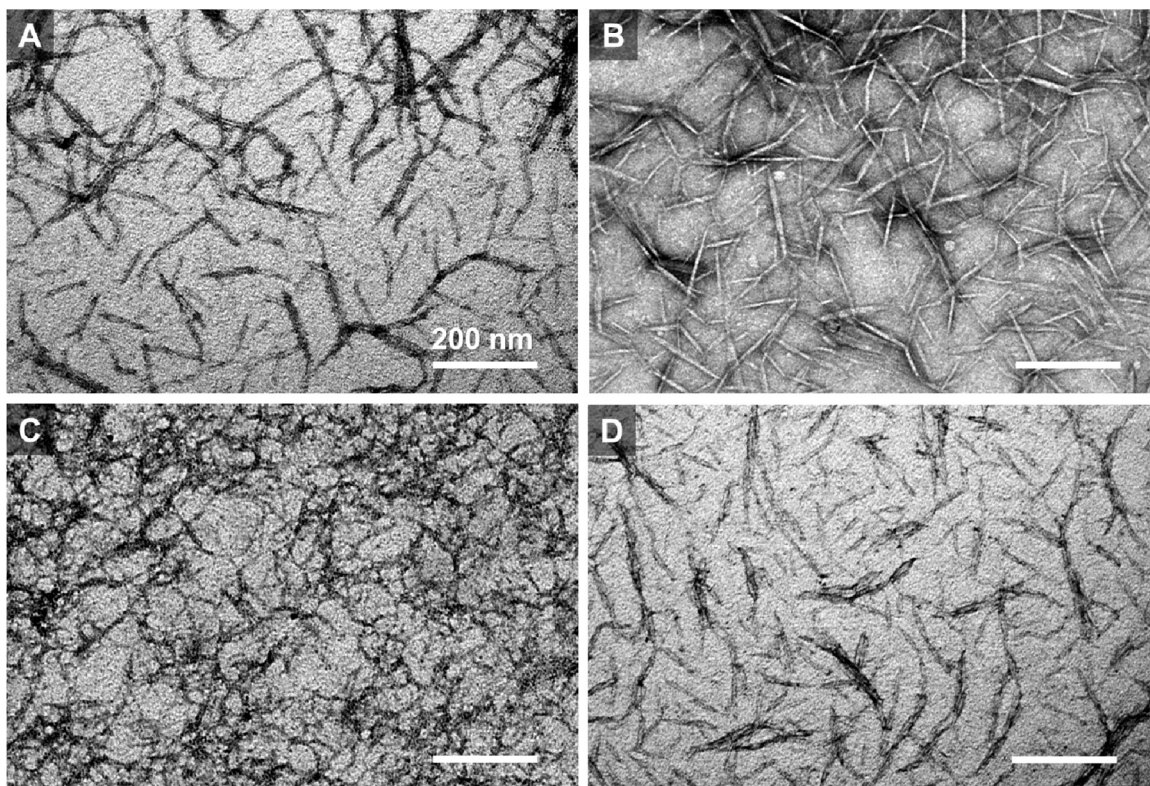
Fig. 25. Transmission electron microcopy (TEM) images of cellulose II nanocrystals (CNCs) prepared from mercerized wood cellulose (A), mercerized cotton lint (B), regenerated cellulose fiber (C), and regenerated cellulose beads (D) by 4-acetamido-TEMPO/NaClO/NaClO$_2$ oxidation in buffer at pH 4.8 and 60 °C for 3 d and subsequent sonication in water [136]. Mercerization was performed by soaking in 5 M NaOH at room temperature for 1 d. Copyright 2012. Reproduction with permission from Springer Nature.
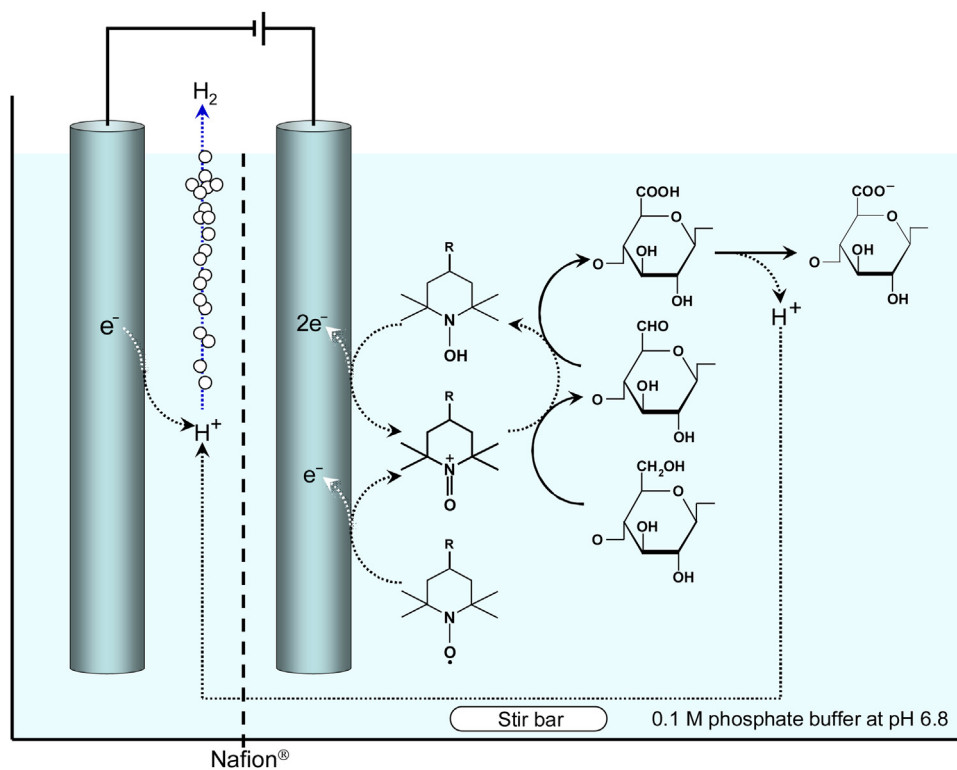
Fig. 26. TEMPO electro-mediated oxidation of cellulose in buffer at pH 6.8 [145]. No chlorine-containing primary oxidant is needed in this system. Copyright 2010. Reproduction with permission from the American Chemical Society.
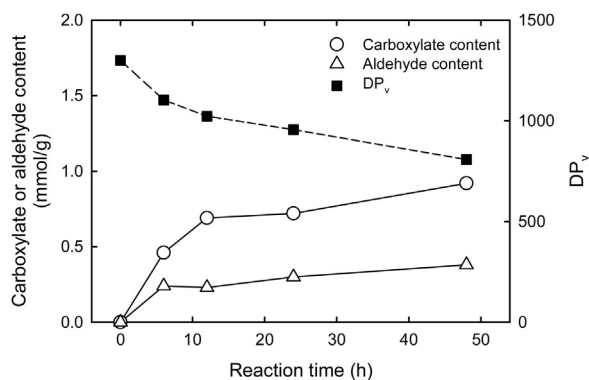
Fig. 27. Relationship between reaction time of wood cellulose by TEMPO electro-mediated oxidation in buffer at pH 6.8 and carboxylate or aldehyde contents and viscosity-average degree of polymerization (DP$_v$) of oxidized celluloses [147]. Copyright 2011. Reproduction with permission from Springer Nature.

diates, to C6-carboxy groups during TEMPO/NaBr/NaClO oxidation. Not only NaClO and/or NaBrO but also TEMPO$^+$ molecules can, therefore, oxidize C6-aldehyde groups to C6-carboxylate groups, as shown in Fig. 3 in the 2nd chapter.

When water-insoluble curdlan, amylodextrin, and regenerated cellulose fiber are used in electro-mediated oxidation with 4-AcNH-TEMPO in a buffer at pH 6.8, more than 90% of the C6–OH groups of curdlan and amylodextrin are oxidized to sodium C6-carboxylate groups to form corresponding water-soluble sodium polyuronates [145]. Molar masses of the oxidized products prepared are much higher than those prepared from the same polysaccharides by the TEMPO/NaBr/NaClO system in water at pH 10. When a regenerate cellulose fiber (viscose rayon) is treated by TEMPO electro-mediated oxidation in a buffer at pH 6.8 and room temperature for 45 h, sodium C6-carboxylate and C6-aldehyde groups of 1.1 and 0.6 mmol/g, respectively, are formed in the oxidized cellulose fiber. The fine surface morphology and cellulose II crystal structure of the original viscose rayon are maintained, and nearly no weight losses during the oxidation are observed [145]. The TEMPO electro-mediated oxidation is, therefore, a useful chemical modification for regenerated cellulose fibers. Algal celluloses and cotton fabrics have been applied to TEMPO electro-mediated oxidation, and the oxidized products have been characterized [148–150].

10. Other *N*-oxyl radical-mediated oxidations

10.1. TEMPO/laccase/O$_2$ oxidation

The TEMPO/laccase/O$_2$ system in a buffer at pH 4.5 is advantageous, because no chorine-containing oxidant is used [151]. The optimum conditions for wood cellulose to prepare TOCs with high sodium C6-carboxylate contents have been studied. However, laccase molecules are degraded by oxidized TEMPO or TEMPO$^+$ molecules formed by laccase-mediated oxidation with O$_2$, which competes with the oxidation of C6–OH groups in wood cellulose. Consequently, large amounts of laccase and TEMPO, and long reaction times are needed to introduce sodium C6-carboxylate groups of ≈0.6 mmol/g to wood cellulose. The TEMPO/laccase/O$_2$ system undergoes a one-way reaction from TEMPO to reduced TEMPO through TEMPO$^+$ without reconversion to TEMPO [152]. When the TEMPO/laccase/O$_2$ oxidation is repeated to oxidize and then isolated/purified TOC, the amount of sodium C6-carboxylate groups increases to ≈1.1 mmol/g, which is sufficient for conversion of the TOC to TOCNs by sonication in water. However, the higher the carboxylate content of the TOCs, the lower their DP$_v$ values.
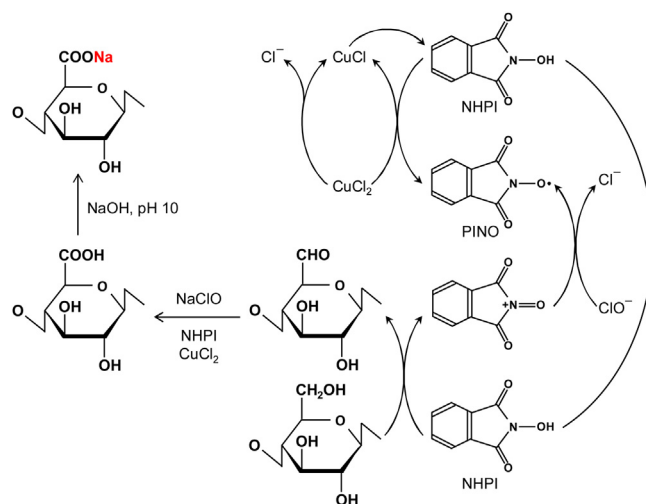
Fig. 28. *N*-Hydroxyphthalimide (NHPI)/co-catalyst/NaClO oxidation of cellulose in water at pH 10 [157].

Because the TEMPO/laccase/O$_2$ oxidation in water under neutral conditions efficiently introduces C6-aldehyde groups together with C6-carboxylate groups to cellulose, this oxidation has been used to improve wet strengths of cellulose sheets by formation of interfiber hemiacetal linkages [153–156].

10.2. N-*Hydroxyphthalimide/co-catalyst/NaClO oxidation*

Coseri et al. have reported other position-selective and nitroxyl radical-mediated oxidations of regenerated cellulose fiber (viscose rayon) with catalytic amounts of *N*-hydroxyphthalimide, a co-catalyst, and NaClO in water or a water/acetonitrile mixture at pH 10 or 10.5 and room temperature [157–160]. The oxidation proceeds via a phthalimide *N*-oxyl radical intermediate (Fig. 28). The following various co-catalysts have been studied in the *N*-hydroxyphthalimide/NaClO oxidation in terms of the amounts of sodium C6-carboxylate groups introduced to oxidized fibers, crystallinities, and DPs: anthraquinone, Pb(OAc)$_4$, CuCl$_2$, UV irradiation, Ce(NH$_4$)$_2$(NO$_3$)$_6$, and NaBr. Sodium C6-carboxylate groups up to ≈0.3 mmol/g are introduced into the regenerated cellulose fibers, which maintain the original cellulose II crystallinities. However, significant depolymerization is unavoidable during the oxidation; the original DP 235 of the viscose rayon decreases to 40–90 after oxidation.

10.3. TEMPO/Na$_2$SO$_4$/NaClO oxidation

A cotton fabric is oxidized using TEMPO/NaBr/NaClO and TEMPO/Na$_2$SO$_4$/NaClO systems in water at pH 10 under various conditions [78]. Sodium C6-carboxylate contents increase from 0.06 to 0.30–0.44 mmol/g, DP$_v$ values decrease from 2200 to 1000–1220 [161]. The degrees of whiteness reduction of TEMPO-oxidized cotton fabrics after heating are clearly decreased by post-NaBH$_4$ treatment (but not by post-NaClO$_2$ oxidation); small amounts of C2/C3 ketone groups are likely to be present in the oxidized cotton fabrics, resulting in the whiteness reduction after heating. The TEMPO/Na$_2$SO$_4$/NaClO-oxidized cotton fabrics with carboxylate contents of ≈0.3 mmol/g have higher DP$_v$ values and lower degrees of whiteness reduction after heating than those with similar carboxylate contents prepared by the TEMPO/NaBr/NaClO oxidation [161]. The former oxidation system has, therefore, some advantages in terms of suitable functionalization of cotton fabrics as clothing materials without using expensive NaBr. Scanning electron microscopy combined with energy-dispersive X-ray analysis
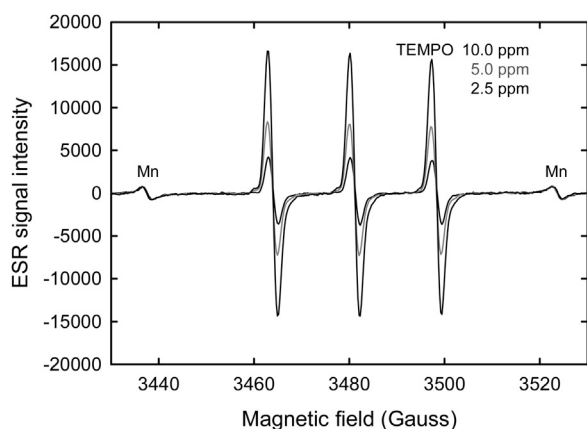
Fig. 29. Representative electron spin resonance (ESR) spectra of aqueous TEMPO solutions with different TEMPO concentrations in water measured using manganese spectrum as an external standard [162].

of the oxidized cotton fibers shows that the TEMPO/Na_2SO_4/NaClO oxidation proceeds homogeneously to the fiber cross section [161]. The TEMPO-oxidized cotton fabrics with sodium C6-carboxylate contents of 0.31–0.32 mmol/g have sufficient burst strength and stiffness values for clothing materials, and deodorizing efficiencies to ammonia and acetic acid gases even after 100 repetitions of laundry treatment. The TEMPO-oxidized cotton fabrics have, therefore, potential application as new functional clothing materials. TEMPO-oxidation behaviour can monitored in terms of time-dependent changes in TEMPO radical concentration of reaction solutions using electron spin resonance (ESR; Fig. 29) [162,163].

10.4. Sonication-assisted TEMPO-mediated oxidation

Sonication-assisted TEMPO-mediated oxidation has been applied to cotton linters, hardwood, bagasse, and palm empty fruit celluloses to efficiently introduce C6-carboxy groups, in which TEMPO or 4-AcNH-TEMPO is used [164–169]. The sonication of celluloses during TEMPO-mediated oxidation enhances nanofibrillation of oxidized celluloses and also formation of CNCs in some cases. TOCNs and TEMPO-oxidized CNCs are, therefore, formed in part and dispersed at the individual nano-element level together with water-insoluble oxidized products in the oxidation mixtures. Isolation and purification processes of these nano-dispersed TOCNs and CNCs from oxidation mixtures are required, separated from TEMPO and other various water-soluble reagents present in the mixtures.

10.5. Other TEMPO-mediated oxidations

Sodium carboxylate groups of 0.9 mmol/g are introduced to xylan-removed hardwood cellulose by the TEMPO/NaClO oxidation in water at pH 9, and the oxidized celluloses are convertible to TOCNs by mechanical disintegration in water [170]. TEMPO/ClO_2 oxidation under neutral conditions [171], 4-AcNH-TEMPO/peracid system [172], and TEMPO/NaBr/$NaIO_4$ system under acidic conditions [173] have been investigated in terms of oxidation efficiency, molar mass, carboxy group content, etc. These alternative TEMPO-mediated oxidations of cellulose have some advantageous points. However, the TEMPO/NaBr/NaClO system in water at pH 10 and TEMPO/NaClO/$NaClO_2$ system in water under acidic–neutral conditions are advantageous to introduce C6-carboxy groups sufficient in amounts for conversion to TOCNs.

11. Side reactions and nanodispersibility of oven-dried TOCs in water

Never-dried and wet TOCs, that are prepared from wood cellulose by the TEMPO/NaBr/NaClO system in water at pH 10 and have sodium C6-carboxylate contents of 1.0–1.7 mmol/g, can be converted to TOCNs with homogeneous widths of ≈3 nm in high nanofibrillation yields by gentle mechanical disintegration in water. However, oven-dried TOCs have low nanodispersibilities even after harsh disintegration in water. When TOCs are reduced with $NaBH_4$ under suitable conditions, almost all C6-aldehydes and C2/C3 ketones present in low amounts are converted to hydroxy groups. The $NaBH_4$-reduced TOCs, even after oven-drying at 105 °C for 3 h, have sufficiently high nanodispersibilities in water in a similar manner to that of never-dried TOCs [174]. Interfibrillar hemiacetal linkages are formed during heating between hydroxy groups and low amounts of either C6-aldehydes or C2/C3 ketones present on crystalline microfibril surfaces of TOCs, resulting in the low nanodispersibilities in water.

The heat-induced discoloration of TOCs is also avoided using $NaBH_4$-reduced TOCs. The C6-aldehydes and C2/C3 ketones present in oven-dried TOCs can be semi-quantitatively measured from the specific UV absorbance spectra at 260 and 290 nm, respectively, for the corresponding TOCN films heated at 105 °C for 3 h [174]. The UV method can, therefore, be used to determine whether TOC samples undergo $NaClO_2$ post-oxidation or $NaBH_4$ post-reduction. Complete position-selectivity cannot, therefore, be achieved for oxidation of C6 − OH groups of native celluloses in the TEMPO/NaBr/NaClO oxidation (Fig. 30) [174].

The continuous reactions of TEMPO/NaBr/NaClO oxidation of wood cellulose and subsequent $NaBH_4$-reduction in a one-pot system in water at pH 10 (without intermediate isolation or purification process) converts the C6-aldehyde and C2/C3 ketone groups to hydroxy groups. The TEMPO-oxidized and $NaBH_4$-reduced TOCs can significantly improve nanodispersibilities in water, even after oven drying, and prevent heat-induced discoloration. The post-oxidation of TOCs with $NaClO_2$ can improve the nanodispersibilities to some extent, although the C2/C3 ketones still remain in the $NaClO_2$-treated TOCs [174].

12. Surface modifications of TOCs and TOCNs

TOCNs are different from other nanocelluloses reported previously in terms of completely individual nanofibers with homogeneous widths of ≈3 nm and the presence of abundant sodium C6-carboxylate groups on the surfaces. The sodium carboxylate groups in TOCs and TOCNs are ion-exchangeable to protonated, and various metal and alkylammonium carboxylate groups in water (Fig. 31) [175–191]. The fibrous TOC-COOH cannot be nanodispersed in water or other organic solvents even by harsh mechanical disintegration. TOCN-COOH nanodispersed in water and some organic solvents such as N,N-dimethylformamide (DMF) and N,N-dimethylacetamide (DMAc) can be prepared from TOCN-COONa once nanodispersed in water with multiple steps [178,179].

Biodegradability/biological stability and hydrophilic/hydrophobic properties of fibrous TOCs and TOCN films are controllable by controlling their counterions [183,184]. The cast/dried TOCN-COONa films have almost no strength in water because of their hydrophilic properties. When the counterions of C6-carboxylate groups in TOCN films are ion-exchanged to Ca^{2+}, Mg^{2+}, Al^{3+}, and Fe^{3+} ions, the obtained TOCN-COOM films (M: metal ions) have sufficient wet-strengths, depending on the metal counterions introduced (Fig. 32A) [189]. The cast/dried TOCN-COONa films decrease in oxygen-barrier properties or increase in oxygen permeabilities at high relative humidity (RH) conditions

Fig. 30. Schematic models of the effects of C6-aldehydes and C2/C3 ketones slightly present in TEMPO-oxidized celluloses on their nanofibrillation behaviour in water after oven-drying [174]. TEMPO-oxidized and then NaBH$_4$-reduced celluloses provide high TOCN yields after disintegration in water because neither C6-aldehydes nor C2/C3 ketones, which form inter-fibrillar hemiacetal linkages during drying, are present in the products. Copyright 2014. Reproduction with permission from Springer Nature.

Fig. 31. Counterion-exchanges of TOCs and TOCNs from sodium ion to protonated, metal, and alkylammonium ions [175–191].

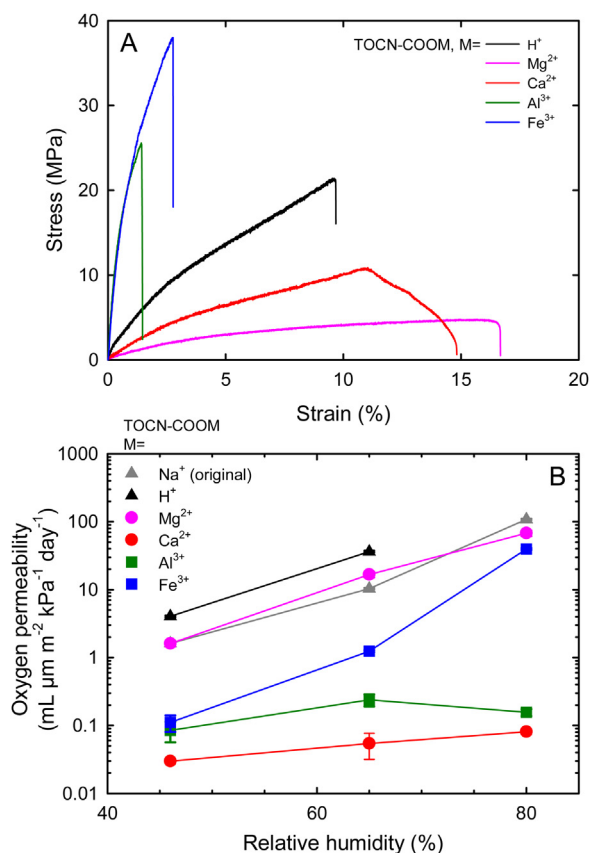**Fig. 32.** Stress–strain curves of wet TOCN–COOM films (A) and oxygen permeabilites of the original TOCN–COONa and counterion-exchanged TOCN–COOM films under various RH conditions (B) [189]. Copyright 2016. Reproduction with permission from Elsevier Ltd.

Fig. 33. Water contact angle of the cast/dried TOCN-COONa, TOCN-COONH$_4$, and TOC-COO$^-$/$^+$NR$_4$ films [188]. Copyright 2014. Reproduction with permission with the American Chemical Society.

because of hydrophilic nature of TOCN-COONa films. When the counterions of TOCN-COONa films are converted to Ca^{2+} and Al^{3+}, the TOCN-COOM films have high oxygen-barrier properties even at high RH conditions (Fig. 32B) [189]. The TOCN-COOAg and TOCN-COOCu films exhibit significant deodorant performance to H$_2$SH and CH$_3$SH gases, which cause serious odor problems in our daily lives [190].

Surface hydrophobization of TOCNs is available by introduction of poly(ethylene)glycol (PEG) chains to almost all carboxylate groups on TOCN surfaces via ammonium salt-type structures, TOCN-COO$^-$/$^+$NH$_3$-CH$_2$CH$_2$-(OCH$_2$CH$_2$)$_n$-OCH$_3$ (TOCN-PEG) (Fig. 31) [186]. Stoichiometric counterion exchange from fibrous TOC-COONa to TOC-COO$^-$/$^+$NR$_4$ is possible by neutralization of the protonated fibrous TOC (TOC-COOH) with quaternary alkylammonium hydroxide (R$_4$N$^+$ OH$^-$) in water. The obtained fibrous TOC-COO$^-$/$^+$NR$_4$ are convertible to transparent and highly-viscous TOCN-COO$^-$/$^+$NR$_4$ dispersions by mechanical disintegration in water and some organic solvents [187,188]. The cast/dried TOCN-COO$^-$/$^+$NR$_4$ films are transparent, flexible, and hydrophobic, depending of the alkyl chain lengths introduced (Fig. 33) [188]. These counterion exchanges in water are characteristic and advantageous surface modifications of TOCs and TOCNs.

13. Differences between TOCN and other nanocelluloses

Various nanocelluloses including cellulose nanofibrils and nanocrystals are prepared from wood cellulose fibers with or without pretreatment followed by mechanical disintegration in water [38,82,102,192,193]. Representative morphologies of TOCNs, conventional CNCs, cellulose nanofibrils prepared only by mechanical
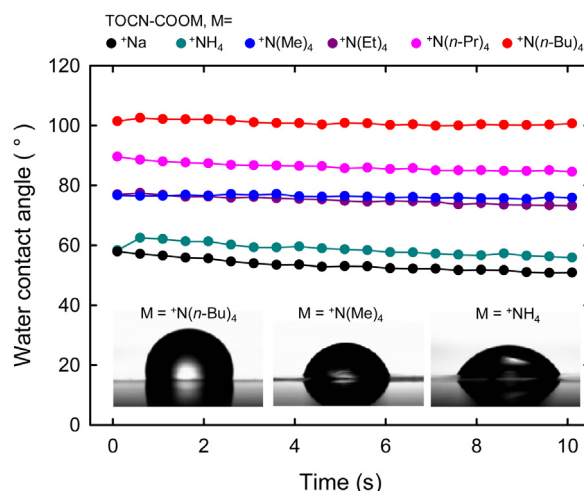
disintegration in water, and microfibrillated celluloses (MFCs) are shown in Fig. 34. Wood CNCs have spindle-like morphologies with heterogeneous widths of 3–15 nm [103]. Cellulose nanofibrils prepared only by mechanical disintegration have heterogeneous widths of 10–50 nm with some branches, and intricate network structures [194]. MFCs contain not only nanofibrils but also micronsized fibers.

Characteristic points of wood TOCNs different from other wood nanocelluloses are as follows. TOCNs are completely individualized nanofibers with homogeneous widths of ≈3 nm and high aspect ratios. TOCNs can be prepared from TOCs with low energy consumption for disintegration in water. TOCNs have carboxylate groups densely, regularly, and position-selectively on their surfaces, and diverse cationic counterions with a variety of functions can be introduced to TOCN surfaces through ion-exchange. TOCNs are convertible to TO-CNCs with the same homogeneous widths and carboxylate contents as those of TOCNs through extended sonication in water.

14. Applications of TOCNs as new bio-based nanomaterials

14.1. Preparations and properties of TOCN bulk materials

Numerous fundamental and application studies on films, fibers, hydrogels, aerogels, foams, and nano-sized network structures prepared from TOCNs have been reported for preparing new bio-based and functional TOCN bulk materials (Fig. 35) [195–216]. Because TOCNs have sodium C6-carboxylate groups densely on crystalline cellulose microfibril surfaces, the TOCN elements form self-assemble and nematic-ordered structures in water and some organic solvents through electric repulsion working between TOCN elements [197]. The characteristic self-assembling structures of TOCNs lead to the formation of various TOCN bulk materials with different properties and functions. When TOCN/water dispersions are cast and dried on a plate, transparent and flexible TOCN films with high mechanical strength, high oxygen-barrier, and low coefficient thermal expansion properties are obtained [195]. These properties are accompanied by nano-layered and highly dense film structures formed from the nematic-ordered TOCN/water dispersions during drying [197,216].

When sodium C6-carboxylate groups of TOCNs are protonated with dilute HCl in TOCN/water dispersions followed by thoroughly washing with water, self-standing TOCN-COOH hydrogels with high stiffness are obtained even at low TOCN
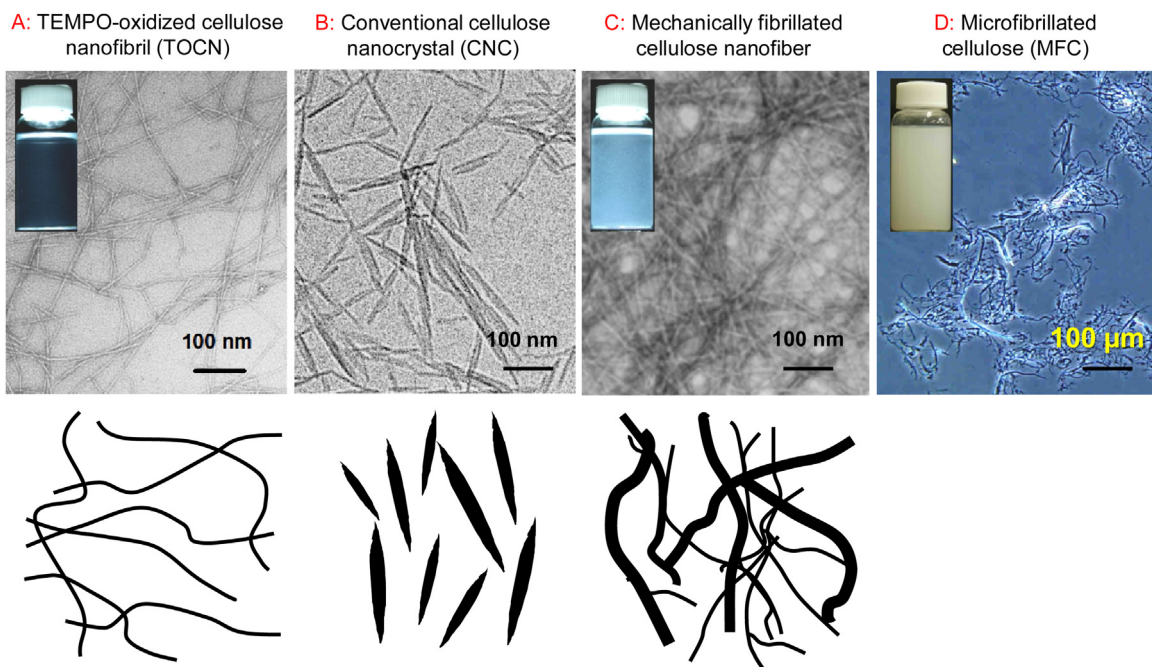
Fig. 34. Transmission electron microscopy images of TEMPO-oxidized wood cellulose nanofibril (A) [81], conventional wood cellulose nanocrystal (B) [103], mechanically fibrillated wood cellulose nanofibril (C) [194], optical microscopy image of microfibrillated wood cellulose (D), and morphology models of A–C. A, B, and C: Copyrights 2007, 1998, and 2003, respectively. Reproduction with permissions with the American Chemical Society, Springer Nature, and Springer Nature, respectively.
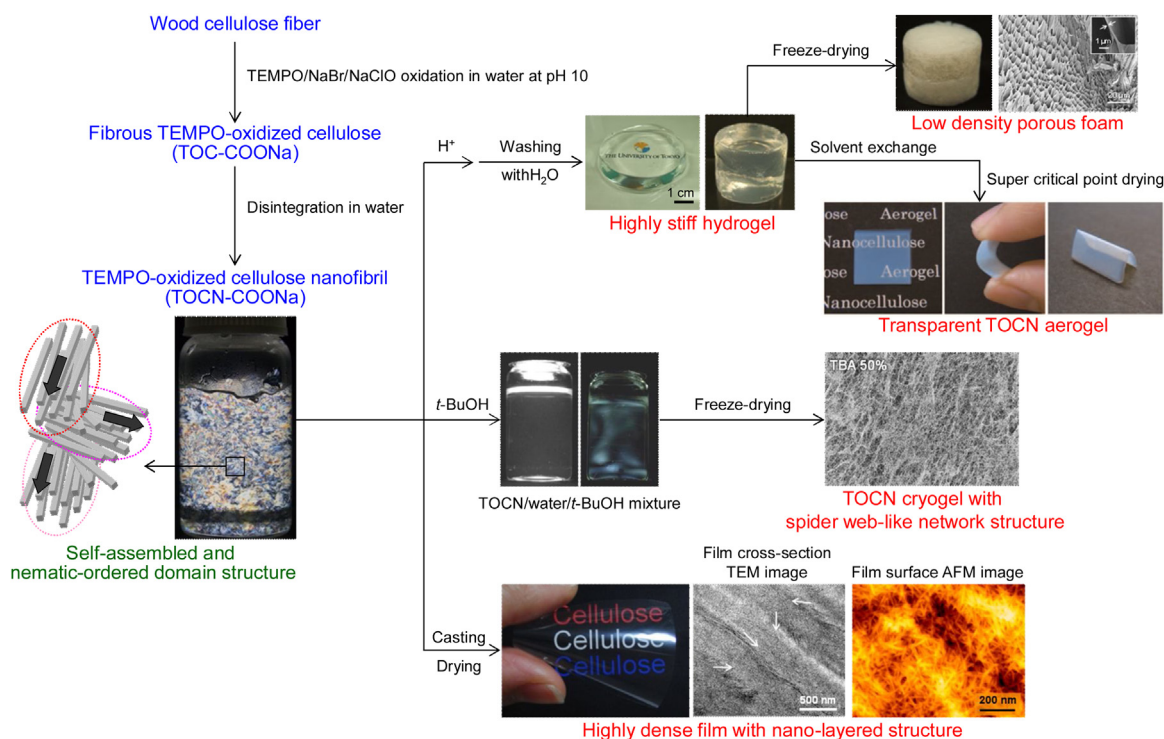
Fig. 35. Preparation of various TOCN bulk materials from TOCN/water dispersions, in which self-assembled and nematic-ordered TOCN structures are present [195–216].

concentrations of $\approx 0.1\%$ [197]. These TOCN-COOH hydrogels are convertible to transparent aerogels with high strength, bendable, and high thermal insulation properties by solvent exchange and subsequent critical point drying [197,199,208]. When TOCN-COONa/water/*tert*-butanol dispersions are freeze-dried, spider web-like network structures with nano-sized pores can be obtained, which are applicable to high performance air filters [201].

14.2. TOCN-containing composite materials

Light-weight and highly strong TOCN-containing composite materials are one of the most promising applications for TOCNs. This is because tensile strengths and Young's moduli of single TOCN elements are ≈ 3 GPa and ≈ 140 GPa, respectively, [112,115] regardless of low densities of ≈ 1.6 g/cm^3. TOCNs are, however, highly hydrophilic, owing to the abundant sodium C6-carboxylate
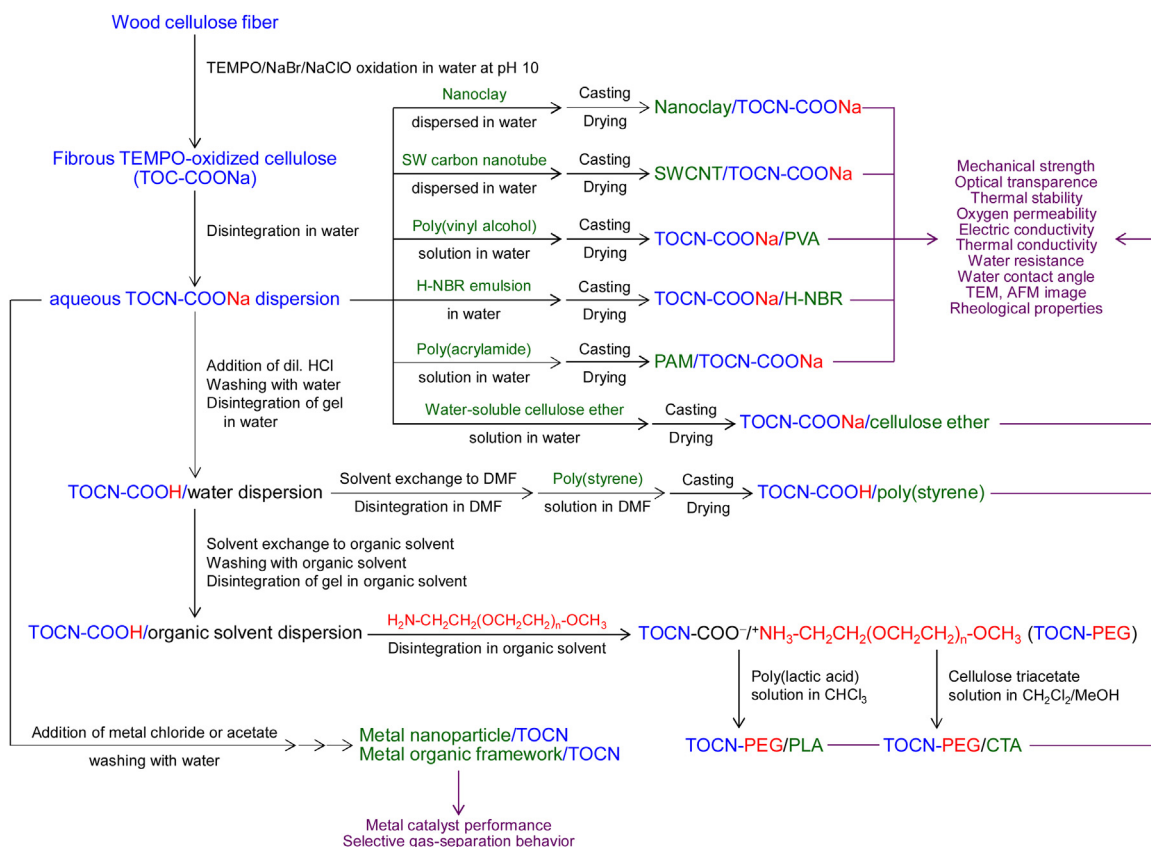
Fig. 36. Preparation of TOCN-containing composite materials [214–228]. TOCN-COONa and various counterion-exchanged TOCNs are used as fillers or matrices of the composites.

groups present on the TOCN surfaces, it is generally difficult to prepare TOCN/polymer composite films, in which hydrophilic TOCN elements are individually dispersed without agglomeration in hydrophobic polymer matrices.

The preparation and characterization of TOCN/polymer or inorganic filler/TOCN composite films have been investigated using poly(vinyl alcohol)[217], poly(acrylamide)[218,219], carbon nanotubes [220], and nanoclays [221,222]. The TOCN-COONa/water dispersions and water-soluble polymers dissolved in water or H-NBR latex dispersed in water were mixed at various weight ratios followed by casting and drying to prepare TOCN/polymer composite films. Single-wall carbon nanotube and nanoclays dispersed in water were mixed with TOCN/water dispersions to prepare composite films at various filler/TOCN weight ratios. Some of them have unique mechanical, transparent, excellent oxygen barrier, thermal, and electric properties, owing to sufficiently nanodispersed TOCN elements or filler nanoparticles without agglomeration in polymer or TOCN matrices, which were supported from their TEM images [220–222].

When metal nanoparticle/TOCN and metal-organic framework/TOCN composites were prepared using the abundant C6-carboxylate groups present on TOCN surfaces as scaffolds, efficient, stable, and recyclable catalysts or selective gas-separation membranes were obtained [177,180,223–225].

Some organic solvents were used to prepare TOCN-containing hydrophobic polymer composite films, such as poly(styrene) [226], poly(lactic acid) (PLA) [186,227], and cellulose triacetate (CTA) [228]. The counterions of TOCN-COONa have to be converted to TOCN-COOH nanodispersible in DMF [178,226] or hydrophobic TOCN-PEG nanodispersible in DMAc, toluene, chloroform, and tetrahydrofuran [186,227,228]. Because poly(styrene) and PLA are soluble in DMF and chloroform, respectively, the TOCN-

COOH/poly(styrene) and TOCN-PEG/PLA composite films were prepared using DMF and chloroform as the media, respectively, by mixing the two components at various weight ratios and successive casting/drying [186,227,228]. The TOCN-PEG/CTA composite films were prepared by mixing the TOCN-PEG/chloroform dispersion and CTA/dichloromethane-methanol (9:1 by vol.) solution at various ratios and subsequent casting/drying [228]. These composite films exhibited significant improvements in mechanical and thermal properties at low TOCN contents. These preparation methods of TOCN/polymer composite films using organic solvents were performed as model experiments to prepare ideal composite films consisting of individually nanodispersed TOCN elements in polymer matrices (Fig. 36).

However, it is difficult to prepare TOCN/polymer composite films consisting of individually nanodispersed TOCN elements through general melt-molding or melt-extrusion processes without using any organic solvent. The TOCN elements initially nanodispersed in water turn to large agglomerates through water-removal process during thermal molding, resulting in almost no improvement in mechanical properties for the TOCN/polymer composites. Another shortcoming for TOCNs is a decrease in thermal degradation temperature from ≈300 °C for the original cellulose to ≈200 °C, which initially occurs through decarboxylation at the abundant carboxylate groups present in TOCNs.

15. Conclusions and future prospects

N-Oxyl radical-mediated oxidation is a unique reaction and has some advantages in terms of efficiency to introduce anionic sodium C6-carboxylate groups to various cellulosic materials under aqueous conditions. The TEMPO/NaBr/NaClO oxidation proceeds

without using any organic solvents, which is different from the conventional cellulose esterifications and etherifications. When native celluloses with cellulose I crystal structures are used as starting materials and TEMPO-mediated oxidation is applied under suitable conditions, the C6–OH groups present on crystalline cellulose microfibril surfaces in native celluloses are position-selectively oxidized to sodium C6-carboxylate groups in TOCs. New cellulose-based nanofibers, TOCNs, with homogeneous widths of $\approx$3 nm and high aspect ratios can be prepared from wood TOCs with sufficient amounts of sodium C6-carboxylate groups by gentle mechanical disintegration in water.

Further efficient surface modifications of TOCs and TOCNs are possible through counterion-exchange of the abundant sodium C6-carobylate groups with protons, various metal and alkylammonium ions [175–191]. Moreover, numerous fundamental and application studies on TOCN bulk materials and TOCN-containing composite materials have been reported to date for preparing new bio-based and functional materials [195–228].

There are some shortcomings in TEMPO-mediated oxidation of cellulose, which have to be solved for further applications of TOCs and TOCNs in industry. Depolymerization should be controlled to prepare TOCs and TOCNs with high DPs and TOCNs with high aspect ratios. If possible, the use of chlorine-containing oxidants such as NaClO and NaClO$_2$ should be avoided because of environmental aspects. The O$_2$, H$_2$O$_2$, O$_3$, or other chlorine-free compounds are preferable as the primary oxidant, if sufficient amounts of sodium C6-carboxylate groups can efficiently be introduced to oxidized celluloses. Safety issues of TEMPO, TOCs, and TOCNs have to be clarified for their industrial production and application. The treatment or recycling of TEMPO or its related compounds present in effluents formed during industrial production of TOCs and TOCNs should be taken into account for establishing environmentally friendly processes of cellulose modification [229,230].

TOCNs and related materials have been commercialized as an ink dispersant of ballpoint pens developed by Daiichi Kogyo Seiyaku and Mitsubishi Pencil since 2013. Nippon Paper Industries and Nippon Paper Crecia have commercialized TOCN-containing disposable diapers for adults with super deodorizing functions that alleviate the burden for care assistants, also since 2013. The world's largest plant to produce TOCNs at a capacity of 500 t/y was installed in the Ishinomaki mill of Nippon Paper Industries, Miyagi, Japan, and TOCN production has started in 2017. Three additional TOCN production plants were installed in Japan (Daiichi-Kogo Seiyaku Co.), Finland (Betulium Oy), and United States (Forest Products Laboratory, Forest Service, United States Department of Agriculture) [231].

TOCs, TOCNs, and their related bulk and composite materials have been developed since 2006, and are, therefore, still new bio-based materials. More fundamental information and data based on experimental and theoretical studies have to be accumulated for further industrial applications of these new materials. The polymer, metal, glass, paper, and other organic and inorganic materials widely used in the present high-tech and commodity fields have long histories of more than several decades. Numerous science and technologies have been accumulated for these materials to be produced and used under the conditions with high reproducibility, runnability, and reliability.

Acknowledgement

References

[1] Lindman B, Karlström G, Stigsson L. On the mechanism of dissolution of cellulose. J Mol Liq 2010;156:76–81.

[2] Medronho B, Romano A, Miguel MG, Stigsson L, Lindman B. Rationalizing cellulose (in)solubility: reviewing basic physicochemical aspects and role of hydrophobic interactions. Cellulose 2012;19:581–7.

[3] Zugenmaier P. Conformation and packing of various crystalline cellulose fibers. Prog Polym Sci 2001;26:1341–471.

[4] Klemm D, Philipp B, Heinze T, Heinze U, Wagenknecht W. Comprehensive cellulose chemistry: fundamentals and analytical methods. Weinheim: Wiley-VCH Verlarg; 2004. p. 9–166.

[5] Atalla RH, Isogai A. Recent developments in spectroscopic and chemical characterization of cellulose. In: Dumitriu S, editor. Polysaccharide. 2nd ed New York: Marcel Dekker; 2005. p. 123–57.

[6] VanderHart DL, Atalla RH. Studies of microstructure in native celluloses using solid-state ^{13}C NMR. Macromolecules 1984;17:1465–72.

[7] Isogai A, Usuda M, Kato T, Uryu T, Atalla RH. Solid-state CP/MAS ^{13}C NMR study of cellulose polymorphs. Macromolecules 1989;22:3168–72.

[8] Fink HP, Weigel P, Purz HJ, Ganster J. Structure formation of regenerated cellulose materials from NMMO-solutions. Prog Polym Sci 2001;26:1473–524.

[9] Rosenau T, Potthast A, Sixta H, Kosma P. The chemistry of side reactions and byproduct formation in the system NMMO/cellulose (lyocell process). Prog Polym Sci 2001;26:1839–919.

[10] Klemm D, Shumann D, Udhardt U, Marsch S. Bacterial synthesized cellulose — artificial blood vessels for microsurgery. Prog Polym Sci 2001;26:1561–603.

[11] Edgar K, Buchanan CM, Debenham JS, Rundquist PA, Seiler BD, Shelton MC, et al. Advances in cellulose ester performance and application. Prog Polym Sci 2001;26:1605–88.

[12] Heinze T, Liebert T. Unconventional methods in cellulose functionalization. Prog Polym Sci 2001;26:1689–762.

[13] Klemm D, Heublein DB, Fink HP, Bohn A. Cellulose: fascinating biopolymer and sustainable raw material. Angew Chem Int Ed 2005;22:3358–93.

[14] Fox SC, Li B, Xu D, Edgar KJ. Regioselective esterification and etherification of cellulose: a review. Biomacromolecules 2011;12:1956–72.

[15] Unruh CC, Kenyon WO. Investigation of the properties of cellulose oxidized by nitrogen dioxide. J Am Chem Soc 1942;64:127–31.

[16] Mercer C, Bolker HI. Keto groups in cellulose and mannan oxidized by dinitrogen tetroxide. Carbohydr Res 1970;14:109–13.

[17] Painter TJ. Preparation and periodate oxidation of C-6-oxycellulose: conformational interpretation of hemiacetal stability. Carbohydr Res 1977;5:95–103.

[18] Bertocchi C, Konowicz P, Signore Z, Zanetti F, Flaibani A, Paoletti S, et al. Synthesis and characterisation of polyglucuronan. Carbohydr Polym 1995;27:295–7.

[19] Zimnitsky DS, Yurkshtovich TL, Bychovsky PM. Synthesis and characterization of oxidized cellulose. J Polym Sci Part A: Polym Chem 2004;42:4785–91.

[20] Gert EV, Torgashov VI, Zubets OV, Kaputskii FN. Preparation and properties of enterosorbents based on carboxylated microcrystalline cellulose. Cellulose 2005;12:517–26.

[21] Peng S, Zheng Y, Wu J, Wu Y, Ma Y, Song W, et al. Preparation and characterization of degradable oxidized bacterial cellulose reacted with nitrogen dioxide. Polym Bull 2012;68:415–23.

[22] Kim UJ, Kuga S, Wada M, Okano T, Kondo T. Periodate oxidation of crystalline cellulose. Biomacromolecules 2000;1:488–92.

[23] Kim UJ, Wada M, Kuga S. Solubilization of dialdehyde cellulose by hot water. Carbohydr Polym 2004;56:7–10.

[24] Calvini P, Gorassini A, Luciano G, Franceschi E. FTIR and WAXS analysis of periodate oxycellulose: evidence for a cluster mechanism of oxidation. Vib Spectrosc 2006;40:177–83.

[25] Potthast A, Kostic M, Schiehser S, Kosma P, Rosenau T. Studies on oxidative modifications of cellulose in the periodate system: molecular weight distribution and carbonyl group profiles. Holzforschung 2007;61:662–7.

[26] Potthast A, Schiehser S, Rosenau T, Kostic M. Oxidative modifications of cellulose in the periodate system — reduction and beta-elimination reactions. Holzforschung 2009;63:12–7.

[27] Sirviö J, Hyväkkö U, Liimatainen H, Niinimäki J, Hormi O. Periodate oxidation of cellulose at elevated temperatures using metal salts as cellulose activators. Carbohydr Polym 2011;83:1293–7.

[28] Calvini S, Gorassini A. Surface and Bulk reactions of cellulose oxidation by periodate. A simple kinetic model. Cellulose 2012;19:1107–14.

[29] Yang H, Tejado A, Alam N, Antal M, van de Ven TGM. Films prepared from electrosterically stabilized nanocrystalline cellulose. Langmuir 2012;28:7834–42.

[30] Liimatainen H, Visanko M, Sirviö JA, Hormi O, Niinimäki J. Enhancement of the nanofibrillation of wood cellulose through sequential periodate–chlorite oxidation. Biomacromolecules 2012;13:1592–7.

[31] Visanko M, Liimatainen H, Sirviö JA, Haapala A, Sliz R, Niinimäki J, et al. Porous thin film barrier layers from 2,3-dicarboxylic acid cellulose nanofibrils for membrane structures. Carbohydr Polym 2014;102:584–9.

[32] de Nooy AEJ, Besemer AC, van Bekkum H. Highly selective nitroxyl radical-mediated oxidation of primary alcohol groups in water-soluble glucans. Carbohyd Res 1995;269:89–98.

[33] Ames BN, McCaan J, Yamasaki E. Methods for detecting carcinogens and mutagens with the salmonella/mammalian-microsome mutagenicity test. Mutat Res Environ Mutat 1975;31:347–63.

[34] de Nooy AEJ, Besemer AC, van Bekkum H. Selective oxidation of primary alcohols mediated by nitroxyl radical in aqueous solution. Kinetics and mechanism. Tetrahedron 1995;51:8023–32.

[35] de Nooy AEJ, Besemer AC, van Bekkum H. On the use of stable organic nitroxyl radicals for the oxidation of primary and secondary alcohols. Synthesis 1996:1153–74.

[36] Bailey WF, Bobbitt JM, Wiberg KB. Mechanism of the oxidation of alcohols by oxoammonium cations. J Org Chem 2007;72:4504–9.

[37] Goldstein S, Samuni A. Kinetics and mechanism of peroxyl radical reactions with nitroxides. J Phys Chem 2007;111:1066–72.

[38] Isogai A, Saito T, Fukuzumi H. TEMPO-oxidized cellulose nanofibers. Nanoscale 2011;3:71–85.

[39] Isogai A, Kato Y. Preparation of polyuronic acid from cellulose by TEMPO-mediated oxidation. Cellulose 1998;5:153–64.

[40] Tahiri C, Vignon MR. TEMPO-oxidation of cellulose: synthesis and characterisation of polyglucuronans. Cellulose 2000;7:177–88.

[41] Isogai T, Yanagisawa M, Isogai A. Degrees of polymerization (DP) and DP distribution of cellouronic acids prepared from alkali-treated celluloses and ball-milled native celluloses by TEMPO-mediated oxidation. Cellulose 2009;16:117–27.

[42] Ibert M, Marsais F, Merbouh N, Brückner C. Determination of the side-products formed during the nitroxide-mediated bleach oxidation of glucose to glucaric acid. Carbohydr Res 2002;337:1059–61.

[43] Shibata I, Isogai A. Depolymerization of cellouronic acid during TEMPO-mediated oxidation. Cellulose 2003;10:151–8.

[44] Coseri S. Cellulose: To depolymerize. . . or not to? Biotechnol Adv 2017;35:251–66.

[45] Muzzarelli RAA, Muzzarelli C, Cosani A, Terbojevich M. 6-Oxychitins, novel hyaluronan-like regiospecifically carboxylated chitins. Carbohydr Polym 1999;39:361–7.

[46] Muzzarelli RAA, Miliani M, Cartolari M, Tarsi R, Tosi G, Muzzarelli C. Polyuronans obtained by regiospecific oxidation of polysaccharides from aspergillus niger, *Trichoderma reesei* and *Saprolegnia sp*. Carbohydr Polym 2000;43:55–61.

[47] Kato Y, Kaminaga J, Matsuo R, Isogai A. TEMPO-mediated oxidation of chitin, regenerated chitin and n-acetylated chitosan. Carbohydr Polym 2004;58:421–6.

[48] Kato Y, Matsuo R, Isogai A. Oxidation process of water-soluble starch in TEMPO-mediated system. Carbohydr Polym 2003;51:69–75.

[49] Delattre C, Rios L, Laroche C, Be NHT, Lecerf D, Picton L, et al. Production and characterization of new families of polyglucuronic acids from TEMPO−NaOCl oxidation of curdlan. Int J Biol Macromol 2009;45:458–62.

[50] Tamura N, Wada M, Isogai A. TEMPO-mediated oxidation of (1→3)-β-D-glucans. Carbohydr Polym 2009;77:300–5.

[51] Guillaume P, Christine G, Traikia M, Michaud P, Redouan E, Isogai A. Antioxidant activities of a polyglucuronic acid sodium salt obtained from TEMPO-mediated oxidation of xanthan. Carbohydr Polym 2015;116:34–41.

[52] Saito T, Yanagisawa M, Isogai A. TEMPO-mediated oxidation of native cellulose: SEC−MALLS analysis of water-soluble and -insoluble fractions in the oxidized products. Cellulose 2005;12:305–15.

[53] Saito T, Isogai A. TEMPO-mediated oxidation of native cellulose. The effect of oxidation conditions on chemical and crystal structures of the water-insoluble fractions. Biomacromolecules 2004;5:1983–9.

[54] Montanari S, Roumani M, Heux L, Vignon MR. Topochemistry of carboxylated cellulose nanocrystals resulting from TEMPO-mediated oxidation. Macromolecules 2005;38:1665–71.

[55] Sang X, Qin C, Tong Z, Kong S, Jia Z, Wan G, et al. Mechanism and kinetics studies of carboxyl group formation on the surface of cellulose fiber in a TEMPO-mediated system. Cellulose 2017;24:2415–25.

[56] Dai L, Long Z, Lv Y, Zhang D, Deng HB, Liu Q. TEMPO-mediated oxidation of cellulose in carbonate buffer solution. Fiber Polym 2015;16:319–25.

[57] Battista OA. Hydrolysis and crystallization of cellulose. Ind Eng Chem 1950;42:502–7.

[58] Battista OA, Coppick S, Howsmon JA, Morehead FF, Sisson WA. Level-off degree of polymerization. Ind Eng Chem 1956;48:333–5.

[59] Håkansson H, Ahlgren P. Acid hydrolysis of some industrial pulps: effect of hydrolysis conditions and raw material. Cellulose 2005;12:177–83.

[60] Shinoda R, Saito T, Okita Y, Isogai A. Relationship between length and degree of polymerization of TEMPO-oxidized cellulose nanofibrils. Biomacromolecules 2012;13:842–9.

[61] Okita Y, Saito T, Isogai A. Entire surface oxidation of various cellulose microfibrils by TEMPO-mediated oxidation. Biomacromolecules 2010;11:1696–700.

[62] Hirota M, Furihata K, Saito T, Kawada T, Isogai A. Glucose/glucuronic acid alternating co-polysaccharides prepared from TEMPO-oxidized native celluloses by surface peeling. Angew Chem Int Ed 2010;49:7670–2.

[63] Sjöstedt A, Wohlert J, Larsson PT, Wågberg L. Structural changes during swelling of highly charged cellulose fibres. Cellulose 2015;22:2943–53.

[64] Su Y, Burger C, Ma H, Chu B, Hsiao BS. Morphological and property investigations of carboxylated cellulose nanofibers extracted from different biological species. Cellulose 2015;22:3127–35.

[65] Su Y, Burger C, Ma H, Chu B, Hsiao BS. Exploring the nature of cellulose microfibrils. Biomacromolecules 2015;16:1201–9.

[66] Mao Y, Liu K, Zhan C, Geng L, Chu B, Hsiao BS. Characterization of nanocellulose using small-angle neutron, X-ray, and dynamic light scattering techniques. J Phys Chem B 2017;121:1340–50.

[67] Sbiai A, Kaddami H, Sautereau H, Maazouz H, Fleury E. TEMPO-mediated oxidation of lignocellulosic fibers from date palm leaves. Carbohydr Polym 2011;86:1445–50.

[68] Ma P, Fu S, Zhai HM. Influence of TEMPO-mediated oxidation on the lignin of thermomechanical pulp. Bioresour Technol 2012;118:607–10.

[69] Lai C, Sheng L, Liao S, Xi T, Zhang Z. Surface characterization of TEMPO-oxidized bacterial cellulose. Surf Interface Anal 2013;45:1673–9.

[70] Pönni R, Pääkkönen T, Nuopponen M, Pere J, Vuorinen T. Alkali treatment of birch kraft pulp to enhance its TEMPO catalyzed oxidation with hypochlorite. Cellulose 2014;21:2859–69.

[71] Eyley S, Thielemans W. Surface modification of cellulose nanocrystals. Nanoscale 2014;6:7764–79.

[72] Hänninen T, Orelma H, Laine J. TEMPO oxidized cellulose thin films analysed by QCM-D and AFM. Cellulose 2015;22:165–71.

[73] Hao J, Xu S, Xu N, Li D, Linhardt RJ, Zhang Z. Impact of degree of oxidation on the physicochemical properties of microcrystalline cellulose. Carbohydr Polym 2017;155:483–90.

[74] Fitz-Binder C, Bechtold T. One-sided surface modification of cellulose fabric by printing a modified tempo-mediated oxidant. Carbohydr Polym 2014;106:142–7.

[75] Sun B, Gu C, Ma J, Liang B. Kinetic study on TEMPO-mediated selective oxidation of regenerated cellulose. Cellulose 2005;12:59–66.

[76] Milanovic J, Kostic M, Milanovic P, Skundric P. Influence of TEMPO-mediated oxidation on properties of hemp fibers. Ind Eng Chem Res 2012;51:9750–9.

[77] Pääkkönen T, Bertinetto C, Pönni R, Tummala GK, Nuopponen M, Vuorinen T. Rate-limiting steps in bromide-free TEMPO-mediated oxidation of cellulose –quantification of the *N*-oxoammonium cation by iodometric titration and UV-vis spectroscopy. Appl Catal A 2015;505:532–8.

[78] Inamochi T, Funahashi R, Nakamura Y, Saito T, Isogai A. Effect of coexisting salt on TEMPO-mediated oxidation of wood cellulose for preparation of nanocellulose. Cellulose 2017;24:4097–101.

[79] Bragd PL, Besemer AC, van Bekkum H. TEMPO-derivatives as catalysts in the oxidation of primary alcohol groups in carbohydrates. J Molec Catal A: Chem 2001;170:35–42.

[80] Saito T, Nishiyama Y, Putaux JL, Vignon M, Isogai A. Homogeneous suspensions of individualized microfibrils from TEMPO-catalyzed oxidation of native cellulose. Biomacromolecules 2006;7:1687–91.

[81] Saito T, Kimura S, Nishiyama Y, Isogai A. Cellulose nanofibers prepared by TEMPO-mediated oxidation of native cellulose. Biomacromolecules 2007;8:2485–91.

[82] Isogai A. Wood Nanocelluloses: fundamentals and applications as new bio-based nanomaterials. J Wood Sci 2013;59:449–59.

[83] Sugiyama J, Vuong R, Chanzy H. Electron diffraction study on the two crystalline phases occurring in native cellulose from an algal cell wall. Macromolecules 1991;24:4168–71.

[84] Woodcock C, Sarko A. Packing analysis of carbohydrates and polysaccharides. 11. Molecular and crystal structure of native ramie cellulose. Macromolecules 1980;13:1183–7.

[85] De Souza Lima MM, Borsali R. Rodlike cellulose microcrystals: structure, properties, and applications. Macromol Rapid Commun 2004;25:771–87.

[86] Kuramae R, Saito T, Isogai A. TEMPO-oxidized cellulose nanofibrils prepared from various plant holocelluloses. React Funct Polym 2015;85:126–33.

[87] Besbes I, Alila S, Boufi S. Nanofibrillated cellulose from TEMPO-oxidized eucalyptus fibres: effect of the carboxyl content. Carbohydr Polym 2011;84:975–83.

[88] Rodionova G, Saito T, Lense M, Eriksen Ø, Gregersen Ø, Fukuzumi H, et al. Mechanical and oxygen barrier properties of films prepared from fibrillated dispersions of TEMPO-oxidized Norway spruce and eucalyptus pulps. Cellulose 2012;19:705–11.

[89] Shi Z, Yang Q, Ono Y, Funahashi R, Saito T, Isogai A. Creation of a new material stream from Japanese cedar resources to cellulose nanofibrils. React Funct Polym 2015;95:19–24.

[90] Zhao Y, Moser C, Lindström ME, Henriksson G, Li J. Cellulose nanofibers from softwood, hardwood, and tunicate: preparation−structure−film performance interrelation. ACS Appl Mater Interfaces 2017;9:13508–19.

[91] Okita Y, Saito T, Isogai A. TEMPO-mediated oxidation of softwood thermomechanical pulp. Holzforschung 2009;63:529–35.

[92] Puangsin B, Yang Q, Saito T, Isogai A. Comparative characterization of TEMPO-oxidized cellulose nanofibril films prepared from non-wood resources. Int J Biol Macromol 2013;59:208–13.

[93] Puangsin B, Soeta H, Saito T, Isogai A. Characterization of cellulose nanofibrils prepared by direct TEMPO-mediated oxidation of hemp bast. Cellulose 2017;24:3767–75.

[94] Benhamou K, Dufresne A, Magnin A, Mortha G, Kaddami H. Control of size and viscoelastic properties of nanofibrillated cellulose from palm tree by varying the TEMPO-mediated oxidation time. Carbohydr Polym 2014;99:74–83.

[95] Soni B, Hassan EB, Mahmound B. Chemical isolation and characterization of different cellulose nanofibers from cotton stalks. Carbohydr Polym 2015;134:581–9.

[96] Du C, Li H, Li B, Liu M, Zahn H. Characteristics and properties of cellulose nanofibers prepared by TEMPO oxidation of corn husk. Bioresources 2016;11:5276–84.

[97] Kekäläinen K, Liimatainen H, Illikainen M, Maloney TC, Niinimäki J. The role of hornification in the disintegration behaviour of TEMPO-oxidized bleached hardwood fibres in a high-shear homogenizer. Cellulose 2014;21:1163–74.

[98] Peyre J, Pääkkönen T, Reza M, Kontturi E. Simultaneous preparation of cellulose nanocrystals and micron-sized porous colloidal particles of cellulose by TEMPO-mediated oxidation. Green Chem 2015;17:808–11.

[99] Bettaieb F, Nechyporchuk O, Khiari R, Mhenni MF, Dufresne A, Belgacem MN. Effect of the oxidation treatment on the production of cellulose nanofiber suspensions from Posidonia oceanica: the rheological aspect. Carbohydr Polym 2015;134:664–72.

[100] Meng Q, Li H, Fu S, Lucia LA. The non-trivial role of native xylans on the preparation of TEMPO-oxidized cellulose nanofibrils. React Funct Polym 2014;85:142–50.

[101] Zhou Y, Saito T, Bergström L, Isogai A. Acid-free preparation of cellulose nanocrystals by TEMPO oxidation and subsequent cavitation. Biomacromolecules 2018;19:633–9.

[102] Habibi Y, Lucia LA, Rojas OJ. Cellulose nanocrystals: chemistry, self-assembly, and applications. Chem Rev 2010;110:3479–500.

[103] Dong XM, Revol JF, Gray DG. Effect of microcrystallite preparation conditions on the formation of colloid crystals of cellulose. Cellulose 1998;5:19–32.

[104] Saito T, Isogai A. Introduction of aldehyde groups on surfaces of native cellulose fibers by TEMPO-mediated oxidation. Colloid Surf A 2006;289:219–25.

[105] Hiraoki R, Fukuzumi H, Ono Y, Saito T, Isogai A. SEC-MALLS analysis of TEMPO-oxidized celluloses using methylation of carboxyl groups. Cellulose 2014;21:164–76.

[106] Ono Y, Ishida T, Soeta H, Saito T, Isogai A. Reliable dn/dc values of cellulose, chitin, and cellulose triacetate dissolved in LiCl/N,N-dimethylacetamide for molecular mass analysis. Biomacromolecules 2016;17:192–9.

[107] Ono Y, Tanaka R, Funahashi R, Takeuchi M, Saito T, Isogai A. SEC−MALLS analysis of ethylenediamine-pretreated native celluloses in LiCl/N,N-dimethylacetamide: Softwood kraft pulp and highly crystalline bacterial, tunicate, and algal celluloses. Cellulose 2016;23:1639–47.

[108] Hiraoki R, Ono Y, Saito T, Isogai A. Molecular mass and molecular-mass distribution of TEMPO-oxidized celluloses and TEMPO-oxidized cellulose nanofibrils. Biomacromolecules 2015;16:675–81.

[109] Lasseuguette E, Roux D, Nishiyama Y. Rheological properties of microfibrillar suspension of TEMPO-oxidized pulp. Cellulose 2008;15:425–33.

[110] Tanaka R, Saito T, Ishii D, Isogai A. Determination of nanocellulose fibril length by shear viscosity measurement. Cellulose 2014;21:1581–9.

[111] Tanaka R, Saito T, Hondo H, Isogai A. Influence of flexibility and dimensions of nanocelluloses on the flow properties of their aqueous dispersions. Biomacromolecules 2015;16:2127–31.

[112] Saito T, Kuramae R, Wohlert J, Berglund LA, Isogai A. An ultrastrong nanofibrillar biomaterial: the strength of single cellulose nanofibrils revealed via sonication-induced fragmentation. Biomacromolecules 2013;14:248–53.

[113] Ahir SV, Huang YY, Terentjev EM. Polymers with aligned carbon nanotubes: active composite materials. Polymer 2008;49:3841–54.

[114] Huang YY, Knowles TPJ, Terentjev EM. Strength of nanotubes, filaments, and nanowires from sonication-induced scission. Adv Mater 2009;21:3945–8.

[115] Iwamoto S, Kai W, Isogai A, Iwata T. Elastic modulus of single cellulose microfibrils from tunicate measured by atomic force microscopy. Biomacromolecules 2009;10:2571–6.

[116] Fukuzumi H, Tanaka R, Saito T, Isogai A. Dispersion stability and aggregation behavior of TEMPO-oxidized cellulose nanofibrils in water as a function of salt addition. Cellulose 2014;21:1553–9.

[117] Jowkarderis L, van de Ven TGM. Rheology of semi-dilute suspensions of carboxylated cellulose nanofibrils. Carbohydr Polym 2015;123:416–23.

[118] Kekäläinen K, Liimatainen H, Biale F, Niinimäki J. Nanofibrillation of TEMPO-oxidized bleached hardwood kraft cellulose at high solids content. Holzforschung 2015;69:1077–88.

[119] Gamelas JAF, Pedrosa J, Lourenço AF, Mutjé P, González I, Chinga-Carrasco G, et al. On the morphology of cellulose nanofibrils obtained by TEMPO-mediated oxidation and mechanical treatment. Micron 2015;72:28–33.

[120] Maloney TC. Network swelling of TEMPO-oxidized nanocellulose. Holzforschung 2015;69:207–13.

[121] Paajanen A, Sonavane Y, Ignasiak D, Ketoja JA, Maloney T, Paavilainen S. Atomistic molecular dynamics simulations on the interaction of TEMPO-oxidized cellulose nanofibrils in water. Cellulose 2016;23:3449–62.

[122] Nechyporchuk O, Belgacem MN, Pignon F. Concentration effect of TEMPO-oxidized nanofibrillated cellulose aqueous suspensions on the flow instabilities and small-angle X-ray scattering structural characterization. Cellulose 2015;22:2197–210.

[123] Iwamoto S, Kai W, Isogai T, Isogai A, Iwata T. Comparison study of TEMPO-analogous compounds on oxidation efficiency of wood cellulose for preparation of cellulose nanofibrils. Polym Degrd Stab 2010;95:1394–8.

[124] Shibuya M, Tomizawa M, Suzuki I, Iwabuchi Y. 2-Azaadamantane N-oxyl (AZADO) and 1-Me-AZADO: highly efficient organocatalysts for oxidation of alcohols. J Am Chem Soc 2006;128:8412–3.

[125] Takaichi S, Isogai A. Oxidation of wood cellulose using 2-azaadamantane N-oxyl (AZADO) or 1-methyl-AZADO catalyst in NaBr/NaClO system. Cellulose 2013;20:1979–88.

[126] Takaichi S, Hiraoki R, Inamochi T, Isogai A. One-step preparation of 2,3,6-tricarboxy cellulose. Carbohydr Polym 2014;110:499–504.

[127] Zhao M, Li J, Mano E, Song Z, Tschaen DM, Grabowski EJJ, et al. Oxidation of primary alcohols to carboxylic acids with sodium chlorite catalyzed by TEMPO and bleach. J Org Chem 1999;64:2564–6.

[128] Saito T, Hirota M, Tamura N, Kimura S, Fukuzumi H, Heux L, et al. Individualization of nano-sized plant cellulose fibrils by direct surface carboxylation using TEMPO catalyst under neutral conditions. Biomacromolecules 2009;10:1992–6.

[129] Saito T, Hirota M, Tamura N, Isogai A. Oxidation of bleached wood pulp by TEMPO/NaClO/NaClO$_2$ system: effect of the oxidation conditions on carboxylate content and degree of polymerization. J Wood Sci 2010;56:227–32.

[130] Tanaka R, Saito T, Isogai A. Cellulose nanofibrils prepared from softwood cellulose by TEMPO/NaClO/NaClO$_2$ systems in water at pH 4.8 or 6.8. Int J Biol Macromol 2012;51:228–34.

[131] Tamura N, Hirota M, Saito T, Isogai A. Oxidation of curdlan and other polysaccharides by 4-acetamide-TEMPO/NaClO/NaClO$_2$ under acid conditions. Carbohydr Polym 2010;81:592–8.

[132] Watanabe E, Tamura N, Saito T, Habu N, Isogai A. Preparation of completely C6-carboxylated curdlan by catalytic oxidation with 4-acetamido-TEMPO. Carbohydr Polym 2014;100:74–9.

[133] Hirota M, Tamura N, Saito T, Isogai A. Oxidation of regenerated cellulose with NaClO$_2$ catalyzed by TEMPO and NaClO under acid-neutral conditions. Carbohydr Polym 2009;78:330–5.

[134] Hirota M, Tamura N, Saito T, Isogai A. Surface carboxylation of porous regenerated cellulose beads by 4-acetamide-TEMPO/NaClO/NaClO$_2$ system. Cellulose 2009;16:841–51.

[135] Hirota M, Tamura N, Saito T, Isogai A. Water dispersion of cellulose II nanocrystals prepared by TEMPO-mediated oxidation of mercerized cellulose at pH 4.8. Cellulose 2010;17:279–88.

[136] Hirota M, Tamura N, Saito T, Isogai A. Cellulose II nano elements prepared from fully mercerized, partially mercerized and regenerated celluloses by 4-acetamido-TEMPO/NaClO/NaClO$_2$ oxidation. Cellulose 2012;19:435–42.

[137] Lai C, Zhang S, Sheng L, Liao S, Xi T, Zhang Z. TEMPO-mediated oxidation of bacterial cellulose in a bromide-free system. Colloid Polym Sci 2013;291:2985–92.

[138] Gehmayr V, Potthast A, Sixta H. Reactivity of dissolving pulps modified by TEMPO-mediated oxidation. Cellulose 2012;19:1125–34.

[139] Tanaka C, Yui Y, Isogai A. TEMPO-mediated oxidation of cotton cellulose fabrics under weakly acidic or neutral conditions. J Fiber Sci Technol 2015;71:191–6.

[140] Belgsir EM, Schäfer HJ. Selective oxidation of carbohydrates on Nafion®–TEMPO-modified graphite felt electrodes. Electrochem Commun 2001;3:32–5.

[141] Liaigre D, Breton T, El Belgsir EM. Kinetic and selectivity control of TEMPO electro-mediated oxidation of alcohols. Electrochem Commun 2005;7:312–6.

[142] Barhdadi R, Comminges C, Doherty AP, Nedelec JY, O'Toole S, Troupel M. The electrochemistry of TEMPO-mediated oxidation of alcohols in ionic liquid. J Appl Electrochem 2007;37:723–8.

[143] Yoshida T, Kuroboshi M, Oshitani J, Gotoh K, Tanaka H. Electroorganic synthesis in oil-in-water nanoemulsion: TEMPO-mediated electrooxidation of amphiphilic alcohols in water. Synlett 2007;17:2691–4.

[144] Comminges C, Barhdadi R, Doherty AP, O'Toole S, Troupel M. Mechanism of 2,2'6,6'-tetramethylpiperidin-N-oxyl-mediated oxidation of alcohols in ionic liquids. J Phys Chem A 2008;112:7848–55.

[145] Isogai T, Saito T, Isogai A. TEMPO electromediated oxidation of some polysaccharides including regenerated cellulose fiber. Biomacromolecules 2010;11:1593–9.

[146] Parpot P, Servat K, Bettencourt AP, Huse H, Kokoh KB. TEMPO mediated oxidation of carbohydrates using electrochemical methods. Cellulose 2010;17:815–24.

[147] Isogai T, Saito T, Isogai A. Wood cellulose nanofibrils prepared by TEMPO electro-mediated oxidation. Cellulose 2011;18:421–31.

[148] Carlsson DO, Lindh J, Strømme M, Mihranyan A. Susceptibility of I$_\alpha$- and i$_\beta$-dominated cellulose to TEMPO-mediated oxidation. Biomacromolecules 2015;16:1643–9.

[149] Carlsson DO, Lindh J, Nyholm L, Strømme M, Mihranyan A. Cooxidant-free TEMPO-mediated oxidation of highly crystalline nanocellulose in water. RSC Adv 2014;4:52289–98.

[150] Jin Y, Edler KJ, Marken F, Scott JL. Voltammetric optimisation of TEMPO-mediated oxidations at cellulose fabric. Green Chem 2014;16:3322–7.

[151] IWCE Arends, Li YX, Sheldon RA. Stabilities and rates in the laccase/TEMPO-catalyzed oxidation of alcohols. Biocatal Biotransform 2006;24:443–8.

[152] Jiang J, Ye W, Liu L, Wang Z, Fan Y, Saito T, et al. Cellulose nanofibers prepared using the TEMPO/laccase/O$_2$ system. Biomacromolecules 2017;18:288–94.

[153] Aracri E, Vidal T. Enhancing the effectiveness of a laccase-TEMPO treatment has a biorefining effect on sisal cellulose fibres. Cellulose 2012;19:867–77.

[154] Zhang D, Liu M, Liu Y, Li H. Characteristics of lignocellulosic fibers from hardwood pulp by laccase-catalyzed TEMPO oxidation. Fiber Polym 2016;17:1330–5.

[155] Yu Y, Wang Q, Yuan J, Fan X, Wang P, Cui L. Hydrophobic modification of cotton fabric with octadecylamine via laccase/TEMPO mediated grafting. Carbohydr Polym 2016;137:549–55.

[156] Quintana E, Roncero MB, Vidal T, Valls C. Cellulose oxidation by laccase-TEMPO treatments. Carbohydr Polym 2017;157:1488–95.

[157] Coseri S, Biliuta G. Bromide-free oxidizing system for carboxylic moiety formation in cellulose chain. Carbohydr Polym 2012;90:1415–9.

[158] Coseri S, Nistor G, Fras L, Strnad S, Harabagiu V, Simionescu BC. Mild and selective oxidation of cellulose fibers in the presence of N-hydroxyphthalimide. Biomacromolecules 2009;10:2294–9.

[159] Biliuta G, Fras L, Strnad S, Harabagiu V, Coseri S. Oxidation of cellulose fibers mediated by nonpersistent nitroxyl radicals. J Polym Sci Part A: Polym Chem 2010;48:4790–9.

[160] Biliuta G, Fras L, Drobota M, Persin Z, Kreze T, Stana-Kleinschk K, et al. Comparison study of TEMPO and phthalimide-N-oxyl (PINO) radicals on oxidation efficiency toward cellulose. Carbohydr Polym 2013;91:502–7.

[161] Yui Y, Tanaka C, Isogai A. Functionalization of cotton fabrics by TEMPO-mediated oxidation. J Fiber Sci Technol 2013;69:222–8.

[162] Yui Y, Tanaka C, Isogai A. Analysis of TEMPO-mediated oxidation of cotton cellulose fabrics through electron spin resonance technique. J Fiber Sci Technol 2014;70:53–8.

[163] Buffa JM, Grela MA, Aranguren MI, Mucchi V. EPR spectroscopy applied to the study of the TEMPO mediated oxidation of nanocellulose. Carbohydr Polym 2016;136:744–9.

[164] Qin ZY, Tong GL, Chin YCF, Zhou JC. Preparation of ultrasonic-assisted high carboxylate content cellulose nanocrystals by TEMPO oxidation. Bioresources 2011;6:1136–46.

[165] Paquin M, Loranger É, Hannaux V, Chabot B, Daneault C. The Use of Weissler Method for scale-up a kraft pulp oxidation by TEMPO-mediated system from a batch mode to a continuous flow-through sonoreactor. Ultrason Sonochem 2013;20:103–8.

[166] Mishra SP, Manent AS, Chabot B, Daneault C. Production of nanocellulose from native cellulose − various options utilizing ultrasound. Bioresources 2012;7:422–36.

[167] Rohaizu R, Wanrosli WD. Sono-assisted TEMPO oxidation of oil palm lignocellulosic biomass for isolation of nanocrystalline cellulose. Ultrason Sonochem 2017;34:631–9.

[168] Rattaz A, Mishra SP, Chabot B, Daneault C. Cellulose nanofibres by sonocatalysed-TEMPO-oxidation. Cellulose 2011;18:585–93.

[169] Zhang K, Sun P, Liu H, Shang S, Song J, Wang D. Extraction and comparison of carboxylated cellulose nanocrystals from bleached sugarcane bagasse pulp using two different oxidation methods. Carbohydr Polym 2016;138:237–43.

[170] Pääkkönen T, Dimic-Misic K, Orelma H, Pönni R, Vuorinen T, Maloney T. Effect of xylan in hardwood pulp on the reaction rate of TEMPO-mediated oxidation and the rheology of the final nanofibrillated cellulose gel. Cellulose 2016;23:277–93.

[171] Pääkkönen T, Pönni R, Dou J, Nuopponen M, Vuorinen T. Activation of TEMPO by ClO$_2$ oxidation of cellulose by hypochlorite −fundamental and practical aspects of the catalytic system−. Carbohydr Polym 2017;174:524–30.

[172] Bragd PL, Besemer AC, van Bekkum H. Selective oxidation of carbohydrates by 4-AcNH-TEMPO/peracid systems. Carbohydr Polym 2002;49:397–406.

[173] Lei M, Hu RJ, Wang YG. Mild and selective oxidation of alcohols to aldehydes and ketones using NaIO$_4$/TEMPO/NaBr system under acidic conditions. Tetrahedron 2006;62:8928–32.

[174] Takaichi S, Saito T, Tanaka R, Isogai A. Improvement of nanodispersibility of oven-dried TEMPO-oxidized celluloses in water. Cellulose 2014;21:4093–103.

[175] Saito T, Isogai A. Ion-exchange behavior of carboxylate groups in fibrous cellulose oxidized by the TEMPO-mediated system. Carbohydr Polym 2005;61:183–90.

[176] Fukuzumi H, Saito T, Okita Y, Isogai A. Thermal stabilization of TEMPO-oxidized cellulose. Polym Degrad Stab 2010;95:1502–8.

[177] Koga H, Tokunaga E, Hidaka M, Umemura Y, Saito T, Isogai A, et al. Topochemical synthesis and catalysis of metal nanoparticles exposed on crystalline cellulose nanofibers. Chem Commun 2010;46:8567–9.

[178] Okita Y, Fujisawa S, Saito T, Isogai A. TEMPO-oxidized cellulose nanofibrils dispersed in organic solvents. Biomacromolecules 2011;12:518–22.

[179] Fujisawa S, Okita Y, Fukuzumi H, Saito T, Isogai A. Preparation and characterization of TEMPO-oxidized cellulose nanofibril films with free carboxyl groups. Carbohydr Polym 2011;84:579–83.

[180] Azetsu A, Koga H, Isogai A, Kitaoka T. Synthesis and catalytic features of hybrid metal nanoparticles supported on cellulose nanofibers. Catalysts 2011;1:83–96.

[181] Fujisawa S, Saito T, Isogai A. Nano-dispersion of TEMPO-oxidized cellulose/aliphatic amine salts in isopropyl alcohol. Cellulose 2012;19:459–66.

[182] Salajková M, Berglund LA, Zhou Q. Hydrophobic cellulose nanocrystals modified with quaternary ammonium salts. J Mater Chem 2012;22:19798–805.

[183] Homma I, Isogai T, Saito T, Isogai A. Degradation of TEMPO-oxidized cellulose fibers and nanofibrils by crude cellulase. Cellulose 2013;20:795–805.

[184] Homma I, Fukuzumi H, Saito T, Isogai A. Effects of carboxyl-group counter-ions on biodegradation behaviors of TEMPO-oxidized cellulose fibers and nanofibril films. Cellulose 2013;20:2505–15.

[185] Shimizu M, Fukuzumi H, Saito T, Isogai A. Preparation and characterization of TEMPO-oxidized cellulose nanofibrils with ammonium carboxylate groups. Int J Biol Macromol 2013;59:99–104.

[186] Fujisawa S, Saito T, Kimura S, Iwata T, Isogai A. Surface engineering of ultrafine cellulose nanofibrils toward polymer nanocomposite materials. Biomacromolecules 2013;14:1541–6.

[187] Shimizu M, Saito T, Isogai A. Bulky Quaternary alkylammonium counterions enhance the nanodispersibility of 2,2,6,6-tetramethylpiperidine-1-oxyl-oxidized cellulose in diverse solvents. Biomacromolecules 2014;15:1904–9.

[188] Shimizu M, Saito T, Fukuzumi H, Isogai A. Hydrophobic, ductile, and transparent nanocellulose films with quaternary alkylammonium carboxylates on nanofibril surfaces. Biomacromolecules 2014;15:4320–5.

[189] Shimizu M, Saito T, Isogai A. Water-resistant and high oxygen-barrier nanocellulose films with interfibrillar cross-linkages formed through multivalent metal ions. J Membr Sci 2016;500:1–7.

[190] Sone A, Saito T, Isogai A. Preparation of aqueous dispersions of TEMPO-oxidized cellulose nanofibrils with various metal counterions and their super deodorant performances. ACS Macro Lett 2016;5:1402–5.

[191] Lavoine N, Bras J, Saito T, Isogai A. Improvement of the thermal stability of TEMPO-oxidized cellulose nanofibrils by heat-induced conversion of ionic bonds to amide bonds. Macromol Rapid Commun 2016;37:1033–9.

[192] Klemm D, Kramer F, Moritz S, Lindström T, Ankerfors M, Gray D, et al. Nanocelluloses: a new family of nature-based materials. Angew Chem Int Ed 2011;50:5438–66.

[193] Moon RJ, Martini A, Nairn J, Simonsen J, Yungblood J. Cellulose nanomaterials review: structure, properties and nanocomposites. Chem Soc Rev 2011;40:3941–94.

[194] Hult EL, Iversen T, Sugiyama J. Characterization of the supermolecular structure of cellulose in wood pulp fibres. Cellulose 2003;10:103–10.

[195] Fukuzumi H, Saito T, Kumamoto Y, Iwata T, Isogai A. Transparent and high gas barrier films of cellulose nanofibers prepared by TEMPO-mediated oxidation. Biomacromolecules 2009;10:162–5.

[196] Iwamoto S, Isogai A, Iwata T. Structure and mechanical properties of wet-spun fibers made from natural cellulose nanofibers. Biomacromolecules 2011;12:831–6.

[197] Saito T, Uematsu T, Kimura S, Enomae T, Isogai A. Self-aligned integration of native cellulose nanofibrils towards producing diverse bulk materials. Soft Matter 2011;7:8804–9.

[198] Silva TCF, Habibi Y, Colodette JL, Elder T, Lucia LA. A fundamental investigation of the microarchitecture and mechanical properties of TEMPO-oxidized nanofibrillated cellulose (NFC)-based aerogels. Cellulose 2012;19:1945–56.

[199] Kobayashi Y, Saito T, Isogai A. Aerogels with 3D ordered nanofiber skeletons of liquid-crystalline nanocellulose derivatives as tough and transparent insulators. Angew Chem Int Ed 2014;53:10394–7.

[200] Jiang F, Hsieh YL. Super water absorbing and shape memory nanocellulose aerogels from TEMPO-oxidized cellulose nanofibrils via cyclic freezing−thawing. J Mater Chem A 2014;2:350–9.

[201] Nemoto J, Saito T, Isogai A. Simple freeze-drying procedure for producing nanocellulose aerogel-containing, high-performance air filters. ACS Appl Mater Interfaces 2015;7:19809–15.

[202] Masruchin N, Park BD, Causin V. Influence of sonication treatment on supramolecular cellulose microfibril-based hydrogels induced by ionic interaction. J Ind Eng Chem 2015;29:265–72.

[203] Syverud K, Pettersen SR, Draget K, Chinga-Carrasco G. Controlling the elastic modulus of cellulose nanofibril hydrogels—scaffolds with potential in tissue engineering. Cellulose 2015;22:473–81.

[204] Masruchin N, Park BD, Causin V, Um IC. Characteristics of TEMPO-oxidized cellulose fibril-based hydrogels induced by cationic ions and their properties. Cellulose 2015;22:1993–2010.

[205] Tarrés Q, Oliver-Ortega H, Llop M, Pèlach MA, Delgado-Aguilar M, Mutjé P. Effective and simple methodology to produce nanocellulose-based aerogels for selective oil removal. Cellulose 2016;23:3077–88.

[206] Seantier B, Bendahou D, Bendahou A, Grohens Y, Kaddami H. Multi-scale cellulose based new bio-aerogel composites with thermal super-insulating and tunable mechanical properties. Carbohydr Polym 2016;138:335–48.

[207] Kuang Y, Chen G, Ming S, Wu Z, Fang Z. Solvent resistance of 2,2,6,6-tetramethylpiperidine-1-oxyl (TEMPO) treated cellulose nanofiber film for flexible electronics. Cellulose 2016;23:1979–87.

[208] Sakai K, Kobayashi Y, Saito T, Isogai A. Partitioned airs at microscale and nanoscale: thermal diffusivity in ultrahigh porosity solids of nanocellulose. Sci Rep 2016;6, 20434/1-7.

[209] Lundahl MJ, Cunha AG, Rojo E, Papageorgiu AC, Rautkari L, Arboleda JC, et al. Strength and water interactions of cellulose I filaments wet-spun from cellulose nanofibril hydrogels. Sci Rep 2016;6, 30965/1-13.

[210] Jiang F, Hsieh YL. Self-assembling of TEMPO oxidized cellulose nanofibrils as affected by protonation of surface carboxyls and drying methods. ACS Sustain Chem Eng 2016;4:1041–9.

[211] Marto?a F, Cochereau T, Dumont PJJ, Orgéas L, Terrien M, Belgacem MN. Cellulose nanofibril foams: links between ice-templating conditions, microstructures and mechanical properties. Mater Des 2016;104:376–91.

[212] Liu P, Oksman K, Mathew AP. Surface adsorption and self-assembly of Cu(II) ions on TEMPO-oxidized cellulose nanofibers in aqueous media. J Colloid Interface Sci 2016;464:175–82.

[213] Toivonen MS, Kurki-Suonio S, Wagermaier W, Hynninen V, Hietala S, Ikkala O. Interfacial polyelectrolyte complex spinning of cellulose nanofibrils for advanced bicomponent fibers. Biomacromolecules 2017;18:1293–301.

[214] Wu CN, Cheng KC. Strong, thermal-stable, flexible, and transparent films by self-assembled TEMPO-oxidized bacterial cellulose nanofibers. Cellulose 2017;24:269–83.

[215] Karim Z, Hakalahti M, Tammelin T, Mathew AP. In situ TEMPO surface functionalization of nanocellulose membranes for enhanced adsorption of metal ions from aqueous medium. RSC Adv 2017;7:5232–41.

[216] Zhao M, Ansari F, Takeuchi M, Shimizu M, Saito T, Berglund LA, et al. Nematic structuring of transparent and multifunctional nanocellulose papers. Nanoscale Horiz 2017;3:28–34.

[217] Endo R, Saito T, Isogai A. TEMPO-oxidized cellulose nanofibril/poly(vinyl alcohol) composite drawn fibers. Polymer 2013;54:935–41.

[218] Kurihara T, Isogai A. Properties of poly(acrylamide)/TEMPO-oxidized cellulose nanofibril composite films. Cellulose 2014;21:291–9.

[219] Kurihara T, Isogai A. Mechanism of TEMPO-oxidized cellulose nanofibril film reinforcement with poly(acrylamide). Cellulose 2015;22:2607–17.

[220] Koga H, Saito T, Kitaoka T, Nogi M, Suganuma K, Isogai A. Transparent, conductive, and printable composites consisting of TEMPO-oxidized nanocellulose and carbon nanotube. Biomacromolecules 2013;14:1160–5.

[221] Wu CN, Saito T, Fujisawa S, Fukuzumi H, Isogai A. Ultrastrong and high gas-barrier nanocellulose/clay-layered composites. Biomacromolecules 2012;13:1927–32.

[222] Wu CN, Yang Q, Takeuchi M, Saito T, Isogai A. Highly tough and transparent layered composites of nanocellulose and synthetic silicate. Nanoscale 2014;6:392–9.

[223] Koga H, Azetsu A, Tokunaga E, Saito T, Isogai A, Kitaoka T. Topological loading of Cu(I) catalysts onto crystalline cellulose nanofibrils for the Huisgen click reaction. J Mater Chem 2012;22:5538–42.

[224] Matsumoto M, Kitaoka T. Ultraselective gas separation by nanoporous metal–organic frameworks embedded in gas-barrier nanocellulose films. Adv Mater 2016;28:1765–9.

[225] Vipin AK, Fugetsu B, Sakata I, Isogai A, Endo M, Li M, et al. Cellulose nanofiber backboned Prussian blue nanoparticles as powerful adsorbents for the selective elimination of radioactive cesium. Sci Rep 2016;6, 37009/1-14.

[226] Fujisawa S, Ikeuchi T, Takeuchi M, Saito T, Isogai A. Superior reinforcement effect of TEMPO-oxidized cellulose nanofibrils in polystyrene matrix: optical, thermal and mechanical studies. Biomacromolecules 2012;13:2188–94.

[227] Fujisawa S, Saito T, Kimura S, Iwata T, Isogai A. Comparison of mechanical reinforcement effects of surface-modified cellulose nanofibrils and carbon nanotubes in PLLA composites. Compos Sci Technol 2014;90:96–101.

[228] Soeta H, Fujisawa S, Saito T, Berglund LA, Isogai A. Low-birefringent and transparent composites of nanocellulose-reinforced cellulose triacetate. ACS Appl Mater Interfaces 2015;7:11041–6.

[229] Tanaka C, Yui Y, Isogai A. Degradation of *N*-oxyl radical compounds by Fenton reaction. J Fiber Sci Technol 2017;73:42–8.

[230] Kuutti L, Pajari H, Rovio S, Kokkonen J, Nuopponen M. Chemical recovery in TEMPO oxidation. Bioresources 2016;11:6550–61.

[231] Isogai A. Development of completely dispersed cellulose nanofibers. Proc Jpn Acad Ser B 2018;94:161–79.